Genetic Dissection of the Vav2-Rac1 Signaling Axis in Vascular Smooth Muscle Cells

Salvatore Fabbiano,[a,b] Mauricio Menacho-Márquez,[a,b] María A. Sevilla,[c] Julián Albarrán-Juárez,[d] Yi Zheng,[e] Stefan Offermanns,[d] María J. Montero,[c] Xosé R. Bustelo[a,b]

Centro de Investigación del Cáncer[a] and Instituto de Biología Molecular y Celular del Cáncer,[b] Consejo Superior de Investigaciones Científicas (CSIC) and University of Salamanca, Campus Unamuno, Salamanca, Spain; Departamento de Fisiología y Farmacología, University of Salamanca, Campus Unamuno, Salamanca, Spain[c]; Department of Pharmacology, Max Planck Institute for Heart and Lung Research, Bad Nauheim, Germany[d]; Division of Experimental Hematology and Cancer Biology, Children's Hospital Research Foundation, Cincinnati, Ohio, USA[e]

Vascular smooth muscle cells (vSMCs) are key in the regulation of blood pressure and the engagement of vascular pathologies, such as hypertension, arterial remodeling, and neointima formation. The role of the Rac1 GTPase in these cells remains poorly characterized. To clarify this issue, we have utilized genetically engineered mice to manipulate the signaling output of Rac1 in these cells at will using inducible, Cre-*loxP*-mediated DNA recombination techniques. Here, we show that the expression of an active version of the Rac1 activator Vav2 exclusively in vSMCs leads to hypotension as well as the elimination of the hypertension induced by the systemic loss of wild-type Vav2. Conversely, the specific depletion of Rac1 in vSMCs causes defective nitric oxide vasodilation responses and hypertension. Rac1, but not Vav2, also is important for neointima formation but not for hypertension-driven vascular remodeling. These animals also have allowed us to dismiss etiological connections between hypertension and metabolic disease and, most importantly, identify pathophysiological programs that cooperate in the development and consolidation of hypertensive states caused by local vascular tone dysfunctions. Finally, our results suggest that the therapeutic inhibition of Rac1 will be associated with extensive cardiovascular system-related side effects and identify pharmacological avenues to circumvent them.

The dynamic regulation of the contractile behavior of vSMCs is one of the main mechanisms used by organisms to maintain blood pressure levels under both physiological and hypertensive conditions (1). Vasoconstriction is mediated primarily by pressor molecules, such as angiotensin II (AngII), catecholamines, endothelins, and eicosanoids. Upon binding to their specific G protein-coupled receptors, these stimuli promote the activation of phospholipase C-β-dependent pathways that, via the elevation of the intracellular Ca^{2+} concentration, favor the stimulation of the myosin light chain (MLC) kinase. This protein in turn induces vSMC contractility via MLC phosphorylation (1) (see Fig. 4A, dark red pathway). Vasoconstrictor G protein-coupled receptors consolidate this process through the inactivation of the negative regulatory MLC phosphatase. This requires the activation of the GTPase RhoA, the subsequent stimulation of Rho-associated protein kinase (Rock), and finally the Rock-dependent inactivation of MLC phosphatase by transphosphorylation (1) (see Fig. 4A, light red pathway). When required, vasodilation can be actively promoted by a number of extracellular ligands that antagonize vasoconstriction-promoting routes in vSMCs. One of the main stimuli involved in such a response is nitric oxide (NO) (2), a gas produced by vascular endothelial cells. Upon diffusion into neighboring vSMCs, NO promotes the direct stimulation of soluble guanylate cyclase, cyclic GMP (cGMP) production, and the cGMP-dependent activation of protein kinase G1 (also known as cGMP kinase I). This kinase eventually inactivates actomyosin contractility through the direct, phosphorylation-mediated inactivation of RhoA (2–4) (see Fig. 4A, dark blue pathway). The signal output of this pathway is further fine-tuned by the hydrolysis of cGMP into GMP by phosphodiesterase type 5 (5) (see Fig. 4A). In addition to blood pressure control, vSMCs participate in a variety of vascular-related processes, including the development of hypertension-dependent and independent pathological states, such as cardiovascular remodeling and neointima formation (1).

RhoA belongs to a large GTPase subfamily that includes, among many others, the widely characterized Rac1 and Cdc42 proteins (6, 7). With the notable exception of RhoA, the role of other Rho subfamily GTPases in vSMCs remains poorly characterized (1). The function of Rac1 is particularly unsettled, since available data support its implication in both vasoconstriction (8–10) and vasodilation (11, 12). In favor of the latter role, we have recently reported using mice with a knockout of Vav2, a phosphorylation-dependent GDP/GTP exchange factor involved in the activation step of Rho family GTPases (13–15), the presence of an NO-Src-Vav2-Rac1-p21-activated kinase signaling pathway in vSMCs that favors vasodilation responses through the p21-activated kinase-dependent inactivation of phosphodiesterase type 5 (see Fig. 4A, light blue pathway) (11). The contradictory roles reported for Rac1 in the contractility behavior of vSMCs can be explained if it triggers different signaling responses depending on the extracellular stimuli and upstream exchange factors engaged. However, since most of the aforementioned studies have been done using overexpression methods in cultured vSMCs, it also is possible that some of the Rac1-dependent functions previously reported are the result of exacerbated, nonphysiological effects elicited by those

ectopically expressed mutants and/or the result of their interference with parallel, Rho GTPase-dependent routes. On the other hand, it also can be argued that the results obtained in $Vav2^{-/-}$ mice derive from concurrent signaling defects present in other cell types. There is more agreement regarding the implication of Rac1 in vSMC-dependent pathological processes, such as hypertension-driven arterial remodeling and neointima formation (1, 10, 16). However, since these data have been obtained using ectopically expressed dominant-negative and constitutively active Rac1 mutants, it is still unknown if they accurately reflect the role of endogenous Rac1 in these processes. To clarify the specific roles of Rac1-dependent routes of vSMCs, we decided to utilize a number of genetically manipulated mice to evaluate the short- and long-term effects that the *in vivo* manipulation of the signaling output of Rac1 and Vav family proteins in vSMCs induced in vascular tone, blood pressure, and a number of vessel-associated pathologies. In addition, we used these animals as tools to address related questions in the field, such as the characterization of the impact that these intrinsic vSMC changes induce in systemic physiological circuits traditionally associated with hypertensive states.

MATERIALS AND METHODS

Animals. The basal OncoVav2 mouse strain was custom made (GenOway) and maintained in a mixed C57BL/6-129SV (75%:25%) genetic background. $Vav2^{-/-}$, $Vav3^{-/-}$, $Vav2^{-/-}$; $Vav3^{-/-}$, $Rac1^{flox/flox}$, and $Cdc42^{flox/flox}$ mice have been described before (17–20). These mice were from a pure C57BL/10 genetic background (Vav family knockout mice) or mixed 129SV4–SVjae-BALB–c-C57BL/6 ($Rac1^{flox/flox}$ mice) and C57BL/6-129SV ($Cdc42^{flox/flox}$) genetic backgrounds. To generate the inducible, vSMC-specific strains, basal *OncoVav2*, $Rac1^{flox/flox}$, and $Cdc42^{flo/flox}$ mice were individually crossed with the $Myh11$-Cre-ER^{T2} transgenic line (C57/BL6 genetic background) (21). The genetic background of the resulting compound lines was not homogenized. The constitutive OncoVav2 mouse strain was generated by crossing the basal strain with transgenic mice expressing constitutively expressed Cre (GenOway). These mice were maintained in a mixed C57BL/6-129SV (75%:25%) genetic background. All animals were kept in the pathogen-free quarantine area of the University of Salamanca and Max Planck Institute for Heart and Lung Research animal facilities. Experiments were performed with male mice at the ages indicated in figure legends. Given the disparity of genetic backgrounds, we used the appropriate control animals of the indicated genetic backgrounds in the experiments. All animal-based experiments have been approved by the Bioethics Committees of the University of Salamanca, CSIC, and Max Planck Institute.

In vivo **gene recombination.** Unless otherwise stated, *in vivo* gene recombination was done in 5-week-old male mice using intraperitoneal injections of tamoxifen (1 mg/day; Sigma) solubilized in corn oil (Sigma) for five consecutive days. As a control, parallel cohorts of mice were injected as described above with just corn oil.

Determination of mRNA abundance. RNA was extracted from either mouse organs or primary vSMCs with TRIzol (Sigma), and the abundance of the indicated transcript was determined by quantitative reverse transcription-PCR (qRT-PCR) using the Script one-step RT-PCR kit (Bio-Rad), the StepOnePlus real-time PCR system (Applied Biosystems), and StepOne software, v2.1 (Applied Biosystems) (22). The expression of the endogenous mouse *P36b4* transcript was used as a normalization control. Primers used were 5′-CAT ACG ACG TCC CAG ACT AC-3′ (forward for mouse *Vav2* cDNA), 5′-GGC ATG ACT GAG GAC GAC AA-3′ (forward for mouse *OncoVav2* cDNA), 5′-ACATCGATGGCTCGCAGAAA-3′ (reverse for both *Vav2* and *OncoVav2* cDNAs), 5′-TAT GGG ACA CAG CTG GAC AA-3′ (forward for mouse *Rac1* cDNA), 5′-ACA GTG GTG TCG CAC TTC AG-3′ (reverse for mouse *Rac1* cDNA), 5′-CCT TCC TGA CAC CTC TCT CG-3′ (forward for mouse *Rac2* cDNA), 5′-GAG CTC AGA CCC TCA CTT GG-3′ (reverse for mouse *Rac2* cDNA), 5′-TGC

CAT CTC CTT TCA GGT GAT-3′ (forward for mouse *Cdc42* cDNA), 5′-CGA AAG CTT CAG CCA GTT GTT-3′ (reverse for mouse *Cdc42* cDNA), 5′-GAA GGA CCT TCG GAA TGA CGA-3′ (forward for mouse *Rhoa* cDNA), 5′-TTC CCA CGT CTA GCT TGC AGA-3′ (reverse for mouse *Rhoa* cDNA), 5′-TTG ATG ATG GAG TGT GGC ACC-3′ (forward for mouse *P36b4* cDNA), and 5′-GTG TTT GAC AAC GGC AGC ATT-3′ (reverse for mouse *P36b4* cDNA). To calculate the copy number of *Rac1* and *Rac2* transcripts in vSMCs, two titration curves were calculated using serial dilutions of known concentrations of plasmids encoding mouse *Rac1* (pNM032) and *Rac2* (pNM007) cDNAs (23).

Isolation, culture, and stimulation of primary vSMCs. Aortas were collected from 2-month-old mice, cleaned to eliminate endothelial cells, adipocytes, and connective tissue, cut in approximately 5- by 5-mm segments, and cultured in Dulbecco's modified Eagle medium (Gibco Life Technologies) supplemented with 10% fetal bovine serum, 2 mM L-glutamine, and antibiotics (100 U/ml penicillin and 100 μg/ml streptomycin; Invitrogen) at 37°C in a 5% CO_2 atmosphere. Culture media were changed every 48 h. After 2 weeks, aorta pieces were removed and primary vSMCs were trypsinized (1× dissociation reagent; Gibco Life Technologies), plated onto new plates, and maintained in standard culture medium as described above. This stage was considered passage 1. To induce the elimination of the *Rac1* allele, passage 1 Myh11-Rac1$^{flox/flox}$ cells were cultured in the presence of 1 μM 4-hydroxytamoxifen (4OHT) in ethanol (Sigma). As a control, parallel cultures were incubated in the presence of vehicle alone. After 48 h, the medium was replaced by standard culture medium. Experiments were performed using passage 2 cells. When required, cells were stimulated with sodium nitroprusside (SNP; 10 μM; Sigma), AngII (1 μM; Sigma), or platelet-derived growth factor (20 ng/ml; Peprotech). In the latter two cases, cells were made quiescent previously by starving them overnight. When indicated, cells were treated with Zaprinast (10 μM; Tocris) for 30 min before SNP addition to cultures.

Determination of the active fraction of Rho GTPases. The amount of GTP-bound RhoA and Rac1 in cell lysates was determined using the Rho G-LISA kit (Cytoskeleton). When indicated, primary vSMCs were challenged with SNP for 60 min prior to cell lysis. Plates were read with a Synergy 4 plate reader (BioTek) with Gen5 software (BioTek).

Hemodynamic studies. Systolic, diastolic, and mean blood pressures were recorded in conscious mice using a noninvasive tail cuff method (CODA; Kent Scientific) (18). The same system was used to record in real time the heart rates of animals. To avoid stress-induced changes in those physiological parameters, we subjected mice to similar manipulations during the week previous to the study in order to familiarize them with the experimental procedure.

Immunoblotting. Total protein lysates from aortas or primary vSMC cultures were obtained and transferred onto nitrocellulose filters as previously described (11, 24). Filters were blotted with antibodies to Rac1 (610651; dilution, 1:1,000; BD Bioscience), phospho-MLC (600-401-416; dilution, 1:1,000; Rockland), MLC (3672; dilution, 1:1,000; Cell Signaling) or tubulin α (CP06; dilution, 1:1,000; Calbiochem). Secondary antibodies were from GE Healthcare.

Histological analyses. Tissues were fixed in 4% paraformaldehyde in phosphate-buffered saline solution, paraffin embedded, cut in 2- to 3-μm sections, and finally stained with hematoxylin and eosin (Sigma). All of these procedures were done by independent personnel of the pathology unit of our center. Aorta media walls and cardiomyocyte areas were quantified with MetaMorph software (Universal Imaging).

Tissue fibrosis determinations. The content of hydroxyproline in tissue was determined with a spectrophotometric method as described previously (18). We calculated total collagen assuming that collagen contains 12.7% hydroxyproline.

In vivo **drug treatments.** Sildenafil (20 mg/kg body weight/day; Pfizer), Nω-nitro-L-arginine methyl ester (L-NAME) (700 mg/liter; Sigma), captopril (100 mg/ml; Sigma), propranolol (25 mg/liter; Sigma), atropine (4 mg/liter; Braun), and doxazosin (30 mg/liter; Pfizer) were added in drinking water for the indicated periods of time. AngII (1.44 mg/kg/day; Sigma)
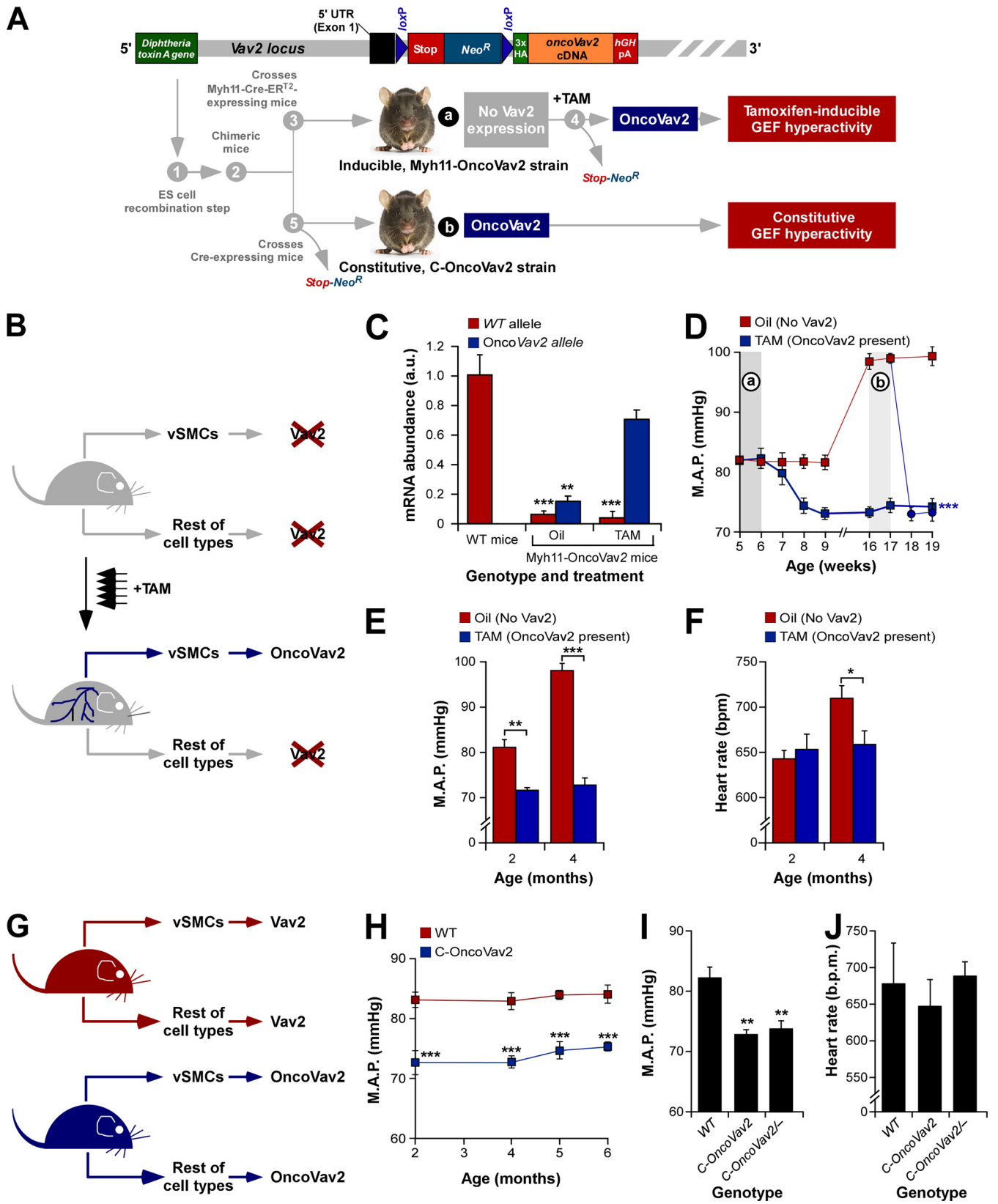
FIG 1 Constitutive activation of Vav2 catalytic activity in vSMCs leads to hypotension. (A) Strategy used to generate the inducible (a) and constitutive (b) *OncoVav2* mouse strains used in this work. The targeting vector is shown at the top. See details in the text. UTR, untranslated region; 3× HA, triple HA epitope; hGHpA, human growth hormone polyadenylation regions; ES, embryonic stem; TAM, tamoxifen. (B) Scheme of the vSMC-specific depletion of Rac1 in Myh11-Rac1$^{flox/flox}$ mice. (C) Abundance of wild-type *Vav2* and *OncoVav2* transcripts in aortas obtained from wild-type (WT) and inducible Myh11-OncoVav2

was administered during 14 days with osmotic pumps (model 1002; Alzet) inserted subcutaneously. When required, AngII and adrenergic receptor inhibitors were combined as described above.

Blood vessel reactivity experiments. Mesenteric beds from exsanguinated animals were dissected and quickly placed in ice-cold Krebs-Henseleit solution (118 mM NaCl, 4.7 mM KCl, 2.5 mM $CaCl_2$, 1.2 mM KH_2PO_4, 1.2 mM $MgSO_4 \cdot 7H_2O$, 25 mM $NaHCO_3$, 11 mM glucose, pH 7.4). Both first- and second-order mesenteric arteries ($\approx$150 μm in diameter) were dissected, and the surrounding connective tissue was eliminated and cut into 2-mm rings. These procedures were done under a stereomicroscope. Two tungsten wires (25 μm in diameter) were introduced through the vessel lumen and mounted on a four-channel myograph (DMT A/S, Denmark) containing 5 ml of Krebs solution at 37°C gassed with carbogen. After a 20-min equilibration period in Krebs solution, the rings were normalized to determine optimal active tension development and standardize experimental conditions. At the start of each experiment, vessel rings were activated with 120 mM K^+, and subsequently the response to serial concentrations of either phenylephrine (10^{-8} to 10^{-4} M) or 5-hydroxytryptamine (10^{-9} to 10^{-5} M) was analyzed. Cumulative concentration-response curves to acetylcholine (10^{-8} to 10^{-4} M) also were performed upon precontraction with 3×10^{-6} M phenylephrine. To compare concentration-response curves, statistical analyses were performed with GraphPad Prism 5.0 software according to the extra-sum-of-squares F test principle.

cGMP production assays. The basal and sodium nitroprusside-induced amounts of cGMP in cultured vSMCs were determined by an enzyme-linked immunosorbent assay (ELISA) kit (cyclic GMP enzyme immunoassay kit; Cayman Chemical) by following the supplier's specifications.

Neointima formation assays. Left-carotid ligation and sample processing were performed as described before (25). Paraffin-embedded samples were stained with orcein (Merck), and neointima formation was quantified with ImageJ software.

In vitro migration and proliferation assays. To measure cell migration, monolayers of primary vSMC in 6-well plates were scratched with a pipette tip and maintained under standard culture conditions. Closure of the wound was measured under the microscope (Zeiss) every 12 h. Wound size was calculated with ImageJ software. Each experiment was performed in triplicate. To facilitate the visualization of cells under microscopy, they were stained with CellTracker green 5-chloromethylfluorescein diacetate (10 μg/ml; Invitrogen) prior to the wound-healing experiment. To measure cell proliferation, cultures of vSMCs maintained in six-well plates were serum starved overnight and, when appropriate, subsequently stimulated with platelet-derived growth factor (20 ng/ml; Peprotech). At the indicated periods of time, the medium was removed and cells maintained for 1 h at 37°C in 100 μl of 3-(4,5-dimethylthiazol-2-yl)-2,5-diphenyltetrazolium bromide (0.5 mg/ml in phosphate-buffered saline solution; Sigma). Upon removal of 3-(4,5-dimethylthiazol-2-yl)-2,5-diphenyltetrazolium bromide, cells were lysed in Dulbecco's modified Eagle medium (Sigma) and absorbance was read at 570 nm using a spectrophotometer (SmartSpec 3000; Bio-Rad).

Analysis of cardiovascular system- and blood-related molecules. We used ELISA-based kits to determine the amount of serotonin (serotonin ELISA kit; IBL), AngII (angiotensin II ELISA kit; SPI Bio), noradrenaline (CatCombi ELISA; IBL), and adrenaline (CatCombi ELISA; IBL) present in the plasma of mice (17, 18, 26). The amount of choline in plasma was determined using the choline-acetylcholine assay kit (Abcam) (26). Plates

were read with a Synergy 4 plate reader and analyzed with Gen5 software. All experiments were performed by following the suppliers' instructions.

Image processing. Images were assembled and processed for final figure presentation using Canvas 9.0.4 (Deneba Systems).

Statistics. Data were analyzed with either a two-tailed Student's *t* test or a one-way analysis of variance (ANOVA) with Bonferroni *post hoc* test (in the case of multiple comparisons). The sample size was chosen to obtain statistically significant conclusions. In the case of experiments involving tamoxifen-inducible mice, mice were randomly picked to carry out the injections with vehicle and tamoxifen. With the exception of immunohistochemical data, the scoring of experiments was not done blindly. No samples were excluded from final analyses. Results with a *P* value of ≤0.05 were considered statistically significant.

RESULTS

The Vav2 route present in vSMCs contributes to blood pressure regulation in a fully autonomous manner. To assess the direct contribution of vSMC-specific Vav2 signaling to blood pressure control, we generated a mouse strain that can express a constitutively active version of Vav2 under the regulation of the endogenous *Vav2* gene promoter in either an inducible or constitutive manner (Fig. 1A). To this end, we used standard genomic recombination techniques to insert an ectopic cassette containing a cDNA fragment encoding a truncated, hemagglutinin (HA)-tagged $Vav2^{\Delta 1-184}$ mutant protein (here termed OncoVav2) downstream of the first exon of the mouse *Vav2* locus. We have shown before that this type of truncated Vav protein shows phosphorylation-independent, constitutive exchange activity due to the removal of the N-terminal inhibitory domains (14, 27–29). To make possible the inducible expression of this protein, this cassette contained 5′-located *Stop-Neo^R* DNA sequences flanked by *loxP* sites (Fig. 1A). Upon the generation of mice containing this mutant *Vav2* locus (Fig. 1A, points 1 and 2), they were crossed with the already-described *Myh11-Cre-ER^{T2}* (21) line to generate the inducible *Myh11-Cre-ER^{T2}*; *Vav2$^{loxP-Stop-NeoR-loxP-HAOncoVav2/loxP-Stop-NeoR-loxP-HAOncoVav2}$* mouse strain (here designated Myh11-OncoVav2) (Fig. 1A, points 3 and a). *Myh11-Cre-ER^{T2}* mice express a fusion protein composed of the Cre recombinase and a mutant version of the estrogen receptor domain (Cre-ER^{T2}) under the regulation of the *Myh11* gene promoter, allowing the Cre-dependent inactivation of desired target genes in vascular, bladder, and intestinal smooth muscle cells when tamoxifen is administered to animals (21). Since this transgene is integrated in the Y chromosome, the recombination step is limited to males (21). Due to the experimental strategy chosen, mouse homozygotes for the mutant *loxP-Stop-Neo^R-loxP-HA-OncoVav2* allele will lack the expression of endogenous wild-type Vav2; therefore, they are expected to behave as standard *Vav2$^{-/-}$* knockout mice (Fig. 1A and B). Upon the tamoxifen-mediated activation of the Cre-ER^{T2} chimera, Onco-Vav2 will be expressed specifically in SMCs due to the removal of the upstream *Stop-Neo^R* sequences (Fig. 1A, point 4, and B). However, the rest of the tissues of these mice will remain Vav2 deficient due to the lack of expression of the Cre-ER^{T2} fusion protein in them

mice treated as indicated. Values are shown relative to the abundance obtained for the wild-type *Vav2* mRNA in aortas from *Vav2$^{+/+}$* animals (which was given an arbitrary value of 1). a.u., arbitrary units. **, $P \le 0.01$; ***, $P \le 0.001$ ($n = 3$). (D to F) Mean arterial pressure (D and E) and heart rate (F) present in control and Myh11-OncoVav2 mice at the indicated ages. In panel D, the two alternative periods of injections with either oil or tamoxifen in normotensic and hypertensive periods of mice are depicted as shaded gray areas and are labeled with a circled "a" and "b," respectively. $P \le 0.05$ (*), $P \le 0.01$ (**), and $P \le 0.001$ (***) relative to oil-injected mice in each injection protocol ($n = 6$). M.A.P., mean arterial pressure; b.p.m., beats per minute. (G) Scheme of the Vav2 expression patterns in wild-type and C-OncoVav2 mice. (H to J) Mean arterial pressure (H and I) and heart rate (J) of 8-week-old mice of the indicated genotypes. C-OncoVav2, mice homozygous for the *OncoVav2* allele; *OncoVav2/−*, mice containing an *OncoVav2* allele and a null *Vav2* allele. **, $P \le 0.01$ compared to values obtained from wild-type mice ($n = 4$). Error bars represent the standard errors of the means (SEM).
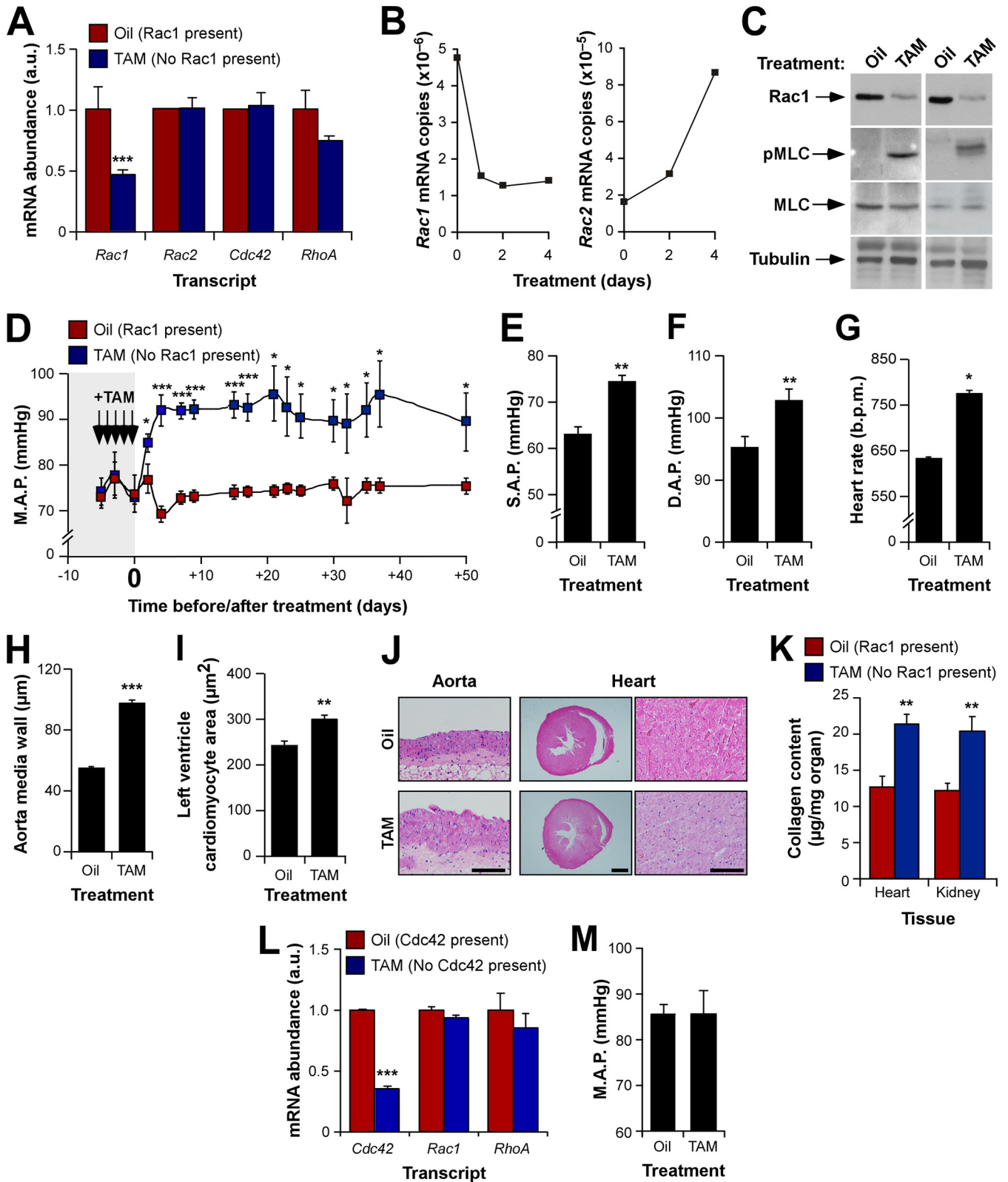
FIG 2 Deletion of Rac1 in vSMCs leads to hypertension and loss of cardiovascular homeostasis. (A) Abundance of the indicated transcripts in aortas obtained from Myh11-Rac1^flox/flox mice 3 weeks after being subjected to injections with either corn oil (Oil) or tamoxifen (TAM). Values obtained for each transcript in control mice were given an arbitrary value of 1. ***, $P \leq 0.001$ relative to the appropriate control ($n = 5$). (B) Changes in the number of copies of *Rac1* (left) and *Rac2* (right) mRNAs in 4OHT-treated primary vSMCs maintained in cell culture. (C) Abundance of the indicated proteins and phosphoproteins (arrows) in total tissue extracts from aortas obtained from Myh11-Rac1^flox/flox mice that were treated as described for panel A. Data obtained in two independent experiments are

(Fig. 1B). Consistent with the planned strategy, we demonstrated, using qRT-PCR, that aortas from Myh11-OncoVav2 mice lack wild-type *Vav2* transcripts and can express the *OncoVav2* mRNA in a tamoxifen-dependent manner (Fig. 1C). As a second experimental model, we generated a mouse line (here designated C-OncoVav2) engineered to express OncoVav2 in all tissues and age periods where the *Vav2* gene is transcriptionally active (Fig. 1A, points 5 and b). Using GTPase-linked immunosorbent assays, we found that the expression of OncoVav2 under these conditions leads to an increase in the basal levels of GTP-bound Rac1 (1.5 ± 0.2 versus the control; $P \leq 0.05$; $n = 3$) and RhoA (1.4 ± 0.1 versus the control; $P \leq 0.05$; $n = 3$) in cultured vSMCs. This dual strategy allowed us to assess the specific contribution of both SMC-specific and ubiquitous Vav2-activated signaling routes to the regulation of vascular tone *in vivo*. In addition, it made it possible to investigate whether the inducible expression of OncoVav2 in vSMCs could counteract the hypertensive effects derived from the systemic loss of wild-type Vav2 (11, 17).

Consistent with the lack of wild-type Vav2 (11, 17), we observed that the noninduced Myh11-OncoVav2 mice develop hypertension (Fig. 1D, red line, and E, red bars) and tachycardia (Fig. 1F, red bars) in an age-dependent manner. However, when the expression of OncoVav2 is induced in vSMCs before the development of the hypertensive state in these animals (Fig. 1D, point a), it progressively promotes a hypotensive state (Fig. 1D, thick blue line, and E, blue bars). Such a phenotype is maintained even at ages when the noninduced Myh11-OncoVav2 mice typically develop a hypertensive state (Fig. 1D, compare the red and thick blue lines) (11, 17). Most notably, the tamoxifen-induced expression of OncoVav2 in vSMCs of mice with full-blown hypertension (Fig. 1D, point b) results in the rapid drop of arterial blood pressure and the acquisition of a hypotensive state (Fig. 1D, compare red and thin blue lines, and E, blue bars). The specific expression of OncoVav2 in SMCs also eliminates the tachycardia exhibited by these mice, leading to heart rates comparable to those found in controls (Fig. 1F, blue bars). All of these alterations are OncoVav2 dependent, because tamoxifen does not trigger them when injected in either female Myh11-OncoVav2 mice (which do not carry the transgene) or in male *Myh11-Cre-ER^T2* mice lacking the *OncoVav2* allele (S. Fabbiano and X. R. Bustelo, unpublished data). The analysis of C-OncoVav2 mice (Fig. 1A and G) revealed the presence of a constitutive hypotensive state from very early postnatal ages (Fig. 1H and I). Such a phenotype is maintained even in mice heterozygous for the *OncoVav2* and null *Vav2* alleles (Fig. 1I), indicating that it can be triggered even with 50% of the normal amount of OncoVav2 protein expressed. The basal heart rate exhibited by C-OncoVav2 mice, however, does not signifi-

cantly change compared to that of the controls (Fig. 1J). Taken together, these results indicate that mice require only the Vav2 route present in vSMCs to ensure full arterial blood pressure control.

Vav2 and Rac1 are commonly involved in blood pressure regulation. Vav2 can activate a number of Rho subfamily GTPases, including Rac1, RhoG, RhoA, and, in reports from some groups, Cdc42 (15). We demonstrated before that $Rhog^{-/-}$ mice do not develop hypertension (17), ruling out the implication of RhoG in Vav2-dependent roles in vascular tone regulation. It also is unlikely that such function is mediated by RhoA, given the well-known implication of this GTPase in vasoconstriction-related vSMC responses (1). To investigate the implication of the remaining GTPases in this signaling route, we generated new mouse strains that allowed the specific, chemically inducible depletion of either Rac1 or Cdc42 in SMCs. To this end, we first crossed the $Myh11$-Cre-ER^{T2} line with the previously described $Rac1^{flox/flox}$ line (30) to establish the compound $Myh11$-Cre-ER^{T2}; $Rac1^{flox/flox}$ line (here referred to as Myh11-Rac1$^{flox/flox}$). Using quantitative RT-PCR analysis, we demonstrated that the injection of tamoxifen in these mice promotes the expected reduction of $Rac1$ transcripts in the aortas of the appropriate strains (Fig. 2A). This effect is specific, since the abundance of transcripts for Rac2, Cdc42, and RhoA does not change in a statistically significant manner under those conditions (Fig. 2A). The addition of 4OHT to *in vitro* cultures of primary vSMCs from male Myh11-Rac1$^{flox/flox}$ mice also results in a rapid, 5-fold reduction in the total abundance of the $Rac1$ transcripts (Fig. 2B, left). In this case, however, we observed a concomitant, 4-fold increase in the number of $Rac2$ mRNA copies present in those cells at late 4OHT administration periods (Fig. 2B, right). Despite such upregulation, the number of copies of this transcript per ng of total RNA under those conditions still is $\approx$60-fold lower than those for the $Rac1$ mRNA in control cells (Fig. 2B). Note that the smaller fold change in the abundance of the $Rac1$ mRNA in aortas than in cultured vSMCs probably is due to the remaining expression of the $Rac1$ gene in endothelial and other cells present in vessels. Using Western blot analyses, we also could demonstrate a marked depletion of the endogenous Rac1 protein in aortas upon the addition of tamoxifen to Myh11-Rac1$^{flox/flox}$ mice (Fig. 2C, upper). Using this mouse model, we found that the inactivation of the $Rac1$ gene promotes the development of high mean (Fig. 2D), systolic (Fig. 2E), and diastolic (Fig. 2F) arterial pressures in Myh11-Rac1$^{flox/flox}$ mice. This hypertension develops quite rapidly upon tamoxifen administration and remains rather stable throughout the rest of the time course analyzed (Fig. 2D). We also observed parallel changes in other cardiovascular param-

shown. Abundance of tubulin α was used as a loading control (bottom panels). p, phosphorylated. (D) Evolution of the mean arterial pressure of Myh11-Rac1$^{flox/flox}$ mice before (shaded area; negative numbers) and after (nonshaded area; positive numbers) five consecutive injections (indicated by arrows) of either oil or tamoxifen. The zero time point indicates the final injection time. $P \leq 0.05$ (*) and $P \leq 0.001$ (***) relative to oil-injected mice ($n = 6$). (E and F) Systolic (S.A.P.) (E) and diastolic (D.A.P.) (F) arterial pressure in Myh11-Rac1$^{flox/flox}$ mice 3 weeks after the indicated treatments. **, $P \leq 0.01$ relative to control mice ($n = 4$). (G) Heart rate of Myh11-Rac1$^{flox/flox}$ mice 3 weeks after the indicated treatments. *, $P \leq 0.05$ relative to oil-injected mice ($n = 6$). (H and I) Mean aorta medium wall size (H) and cell area of left ventricle cardiomyocytes (I) present in Myh11-Rac1$^{flox/flox}$ mice 3 weeks after final oil and tamoxifen injections. **, $P \leq 0.01$ relative to oil-injected mice ($n = 6$). (J) Representative examples of hematoxylin-eosin-stained sections obtained from the indicated tissues of Myh11-Rac1$^{flox/flox}$ mice in the experiment shown in panels G and H. Scale bars, 100 μm. (K) Amount of fibrosis in the indicated tissues from Myh11-Rac1$^{flox/flox}$ mice 3 weeks after final oil and tamoxifen injections. **, $P \leq 0.01$ relative to oil-injected mice ($n = 4$). (L) Abundance of the indicated transcripts in aortas obtained from Myh11-Cdc42$^{flox/flox}$ mice 3 weeks after being subjected to injections with either oil or tamoxifen. Values obtained for each transcript in control mice were given an arbitrary value of 1. ***, $P \leq 0.001$ relative to the appropriate control ($n = 4$). (M) Comparison of the mean arterial pressure of oil- and tamoxifen-treated Myh11-Cdc42$^{flox/flox}$ mice. **, $P \leq 0.01$ relative to control mice ($n = 8$). Error bars represent the SEM. The difference in basal blood pressure between control Myh11-Cdc42$^{flox/flox}$ and Myh11-Rac1$^{flox/flox}$ mice probably is due to their different genetic backgrounds.

eters, including increased amounts of MLC phosphorylation in aortas (Fig. 2C, second row), tachycardia (Fig. 2G), cardiovascular remodeling (Fig. 2H to J), and development of fibrosis in both heart and kidneys (Fig. 2K). Cdc42 does not seem to be involved in this process, because the analysis of tamoxifen-treated *Myh11-Cre-ER^T2^*; *Cdc42^flox/flox^* mice revealed that the vSMC-specific depletion of this GTPase (Fig. 2L) does not have any significant impact on basal blood pressure in mice (Fig. 2M). Taken together, these results indicate that the Vav2-Rac1 signaling axis present in vSMCs has a direct role in the regulation of arterial blood pressure that, depending on how the signal output of the pathway is modified, can lead to either hypotension (when upregulated) or hypertension (when downregulated).

The Vav2-Rac1 pathway is important for acetylcholine-dependent vasodilation responses in vSMCs. To analyze the reactivity of blood vessels in our mouse lines, we investigated the effect of both vasopressor and vasodilation molecules on mesenteric artery rings *ex vivo*. We found that vessels from tamoxifen-treated Myh11-OncoVav2 have slightly increased pressor responses to high concentrations of vasoconstrictor agents, such as phenylephrine (Fig. 3A) and 5-hydroxytryptamine (Fig. 3B). This seems to be a specific feature of OncoVav2-expressing vessels, because the lack of wild-type Vav2 in both standard *Vav2^−/−^* (11) and oil-treated Myh11-OncoVav2 (Fig. 3A and B) does not induce any negative effect in those responses. The physiological impact of this enhanced contractility response does not seem very relevant *in vivo*, since OncoVav2-expressing mice display basal hypotension rather than hypertension (as described above) (Fig. 1D and E). We surmise that this reactivity derives from the OncoVav2-mediated activation of RhoA detected in vSMCs (described above) or, alternatively, a hypotension-associated compensatory mechanism that could have developed in tamoxifen-treated mice. As expected (11), the phenylephrine-precontracted mesenteric arteries from oil-injected Myh11-OncoVav2 mice do show poor relaxation responses to acetylcholine due to the lack of Vav2 expression (Fig. 3C). This molecule triggers NO production in vascular endothelial cells and, subsequently, the NO-dependent stimulation of the soluble guanylate cyclase-cGMP-protein kinase G1 axis that results in the abrogation of RhoA-dependent actomyosin contractility in vSMCs (31). Such a physiological response is restored, although not exacerbated, when OncoVav2 is expressed in those mice (Fig. 3C). Using the same strategy, we observed that mesenteric arteries from control and tamoxifen-treated Myh11-Rac1^flox/flox^ mice exhibit pressor responses similar to those for phenylephrine (Fig. 3D), 5-hydroxytryptamine (Fig. 3E), thromboxane (Fig. 3F), endothelin-1 (Fig. 3G), or AngII (Fig. 3H). In contrast, and similar to results found for aortas from *Vav2^−/−^* knockout mice (11), we observed that phenylephrine-precontracted mesenteric arteries from tamoxifen-treated Myh11-Rac1^flox/flox^ mice do undergo defective relaxation responses to acetylcholine compared to those from control mice (Fig. 3I). These results indicate that the Vav2-Rac1 signaling axis present in vSMCs plays central roles in NO-mediated vasodilation responses in mesenteric arteries. In contrast, it seems to be totally dispensable for contractile responses triggered by a large variety of vasopressor agents. In addition, they indicate that the vasodilatation defects previously detected in *Vav2^−/−^* mice can be attributed to specific signal dysfunctions in vSMCs.

The Vav2-Rac1 pathway is important for the NO-mediated inactivation of RhoA-dependent contractility. We have shown

previously that the vasodilation defects present in arteries of conventional *Vav2^−/−^* knockout mice seemed to stem from improper phosphodiesterase type 5 inactivation during early responses of vSMCs to NO (Fig. 4A, light blue pathway) (11). As a consequence, these cells cannot block the RhoA-Rock2-MLC pathway due to the rapid degradation of the cGMP second messenger by phosphodiesterase type 5 (Fig. 4A) (11). To investigate whether this defect also is present in Rac1-depleted vSMCs, we treated cultures of primary vSMCs from Myh11-Rac1^flox/flox^ mice with 4OHT to induce the Rac1 depletion (as described above) (Fig. 2B) and subsequently evaluated their response to stimulation with a NO donor (SNP) (32). As a control, we utilized cultures of Myh11-Rac1^flox/flox^ vSMCs treated with the vehicle (ethanol) used to prepare the 4OHT solution. After an extra cell passage, we stimulated cells with SNP and measured the production of cGMP using an enzyme-linked immunosorbent assay-based method. Similar to previous results with *Vav2^−/−^* vSMCs (11), we observed that the depletion of Rac1 severely compromises the production of cGMP in SNP-stimulated vSMCs (Fig. 4B). Such a defect is eliminated when vSMCs are treated before the SNP stimulation step with Zaprinast (Fig. 4B), a phosphodiesterase type 5 inhibitor (33). Consistent with these results, we found, using both GTPase-linked immunosorbent and Western blotting, that Rac1-depleted vSMCs cannot trigger the expected reduction in the amount of active RhoA (Fig. 4C) and phospho-MLC (Fig. 4D) that take place during SNP stimulation conditions. Similar defects were seen in SNP-stimulated vSMCs from *Vav2^−/−^* knockout mice (Fig. 4D) (11). These results indicate that the single depletion of either Vav2 or Rac1 protein triggers similar NO-dependent signaling defects in vSMCs. Given these results, we speculated that the expression of OncoVav2 in vSMCs favors a stronger inhibition of phosphodiesterase type 5 under NO stimulation conditions. To test this possibility, we compared both the basal and SNP-induced concentration of cGMP in vSMCs obtained from control and C-OncoVav2 mice. Despite displaying control-like concentrations of cGMP under nonstimulated conditions, we did find that SNP-stimulated OncoVav2-expressing vSMCs promote higher and more sustained amounts of cGMP than control cells (Fig. 4E). However, the expression of OncoVav2 does not seem to achieve full inhibition of phosphodiesterase type 5 catalytic activity, because the amount of cGMP generated by C-OncoVav2 vSMCs can be further increased when Zaprinast is included in these experiments (Fig. 4E).

To corroborate the results described above *in vivo*, we evaluated the effect of the phosphodiesterase type 5 inhibitor sildenafil on the hypertension of tamoxifen-treated Myh11-Rac1^flox/flox^. As a positive control, we carried out parallel experiments with standard *Vav2^−/−^* mice. We have shown before that the hypertension of these mice could be eliminated by the long-term administration of that drug (11). As a negative control, we utilized standard *Vav3^−/−^* knockout mice. The hypertension of these animals is sympathetic based (18, 34); therefore, it cannot be eliminated by the *in vivo* administration of PDE inhibitors (11). We found that the oral administration of sildenafil for just 1 week readily eliminates the hypertension of both tamoxifen-treated Myh11-Rac1^flox/flox^ (Fig. 4F) and standard *Vav2^−/−^* knockout (Fig. 4G) mice. Such an effect is specific, because sildenafil does not affect the basal blood pressure of both oil-treated Myh11-Rac1^flox/flox^ (Fig. 4F) and *Vav2^+/+^* (Fig. 4G) mice. Likewise, it cannot cure the hypertension exhibited by *Vav3^−/−^* mice (Fig. 4G). Also consis-
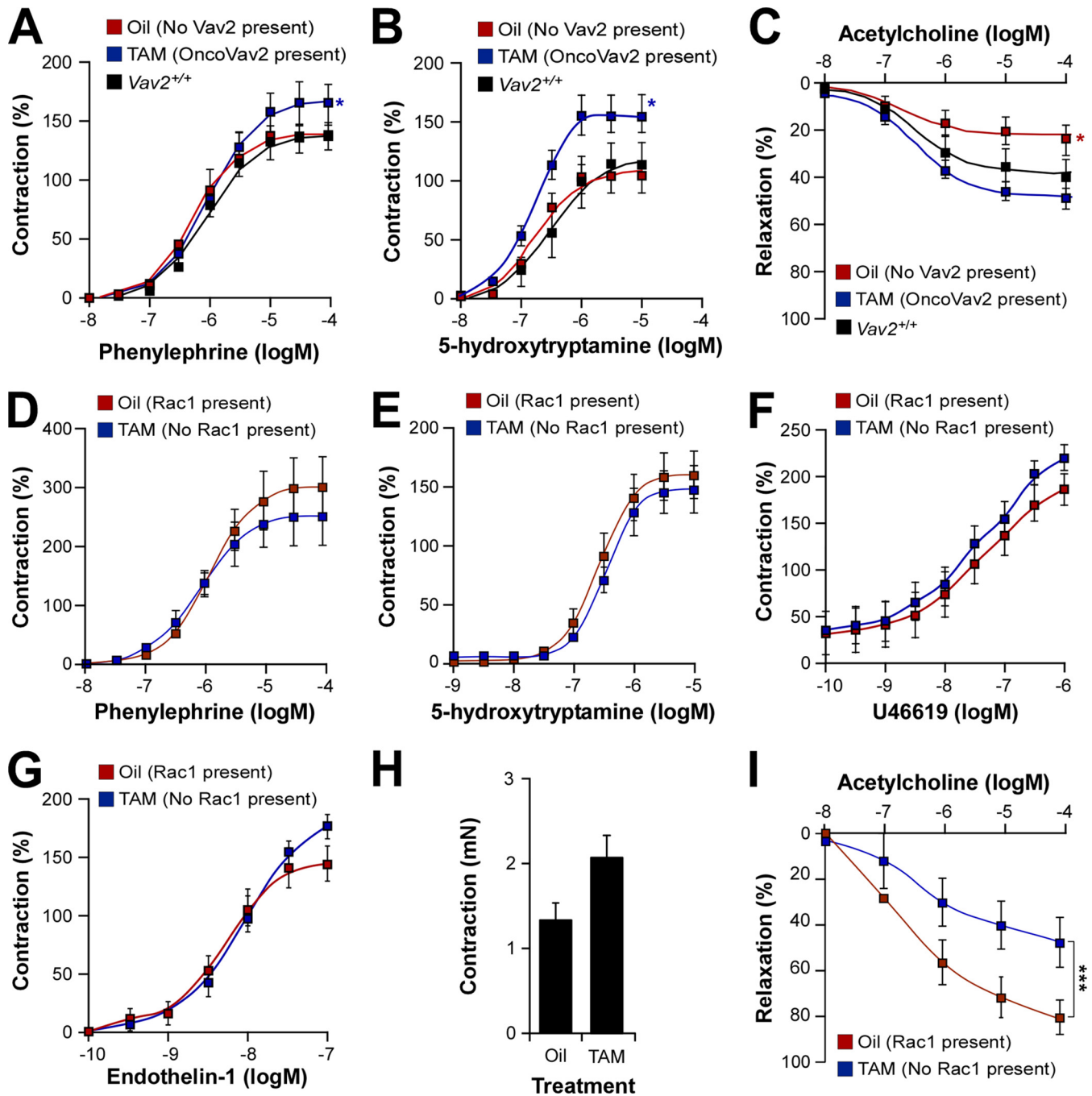
FIG 3 Vav2-Rac1 axis of vSMCs is important for acetylcholine-dependent vasodilation responses. (A and B) Contractile response to the indicated concentrations of phenylephrine (A) and 5-hydroxytryptamine (B) of mesenteric arteries isolated from 2-month-old Myh11-OncoVav2 mice subjected 3 weeks before to injections with either oil or tamoxifen. *, $P \leq 0.001$ for the fit of the concentration-response curves to those for control mesenteric arteries ($n = 4$ and 6 for oil- and tamoxifen-treated mice, respectively). (C) Relaxation response to the indicated concentrations of acetylcholine of mesenteric arteries isolated as indicated for panels A and B. *, $P \leq 0.001$ for the fit of the concentration-response curves to those of control mesenteric arteries ($n = 4$ and 6 for oil- and tamoxifen-treated mice, respectively). (D to G) Contractile response to the indicated concentrations of phenylephrine (D), 5-hydroxytryptamine (E), a thromboxane A_2 receptor agonist (U46619) (F), and endothelin-1 (G) of mesenteric arteries isolated from 2-month-old Myh11-Rac1$^{flox/flox}$ mice that were subjected 3 weeks before to injections with either oil or tamoxifen ($n = 5$ and 9 for oil- and tamoxifen-treated mice, respectively). (H) *Ex vivo* contractile response of mesenteric arteries from oil- and tamoxifen-injected Myh11-Rac1$^{flox/flox}$ mice to a single dose of AngII (1×10^{-7}) ($n = 5$ and 11 for oil- and tamoxifen-treated mice, respectively). (I) Relaxation response to the indicated concentrations of acetylcholine of mesenteric arteries from 2-month-old Myh11-Rac1$^{flox/flox}$ mice that were subjected 3 weeks before to injections with either oil or tamoxifen. ***, $P \leq 0.001$ for the fit of the concentration-response curves to those of control mesenteric arteries ($n = 5$ and 9 for oil-treated tamoxifen-treated mice, respectively). Error bars represent the SEM.
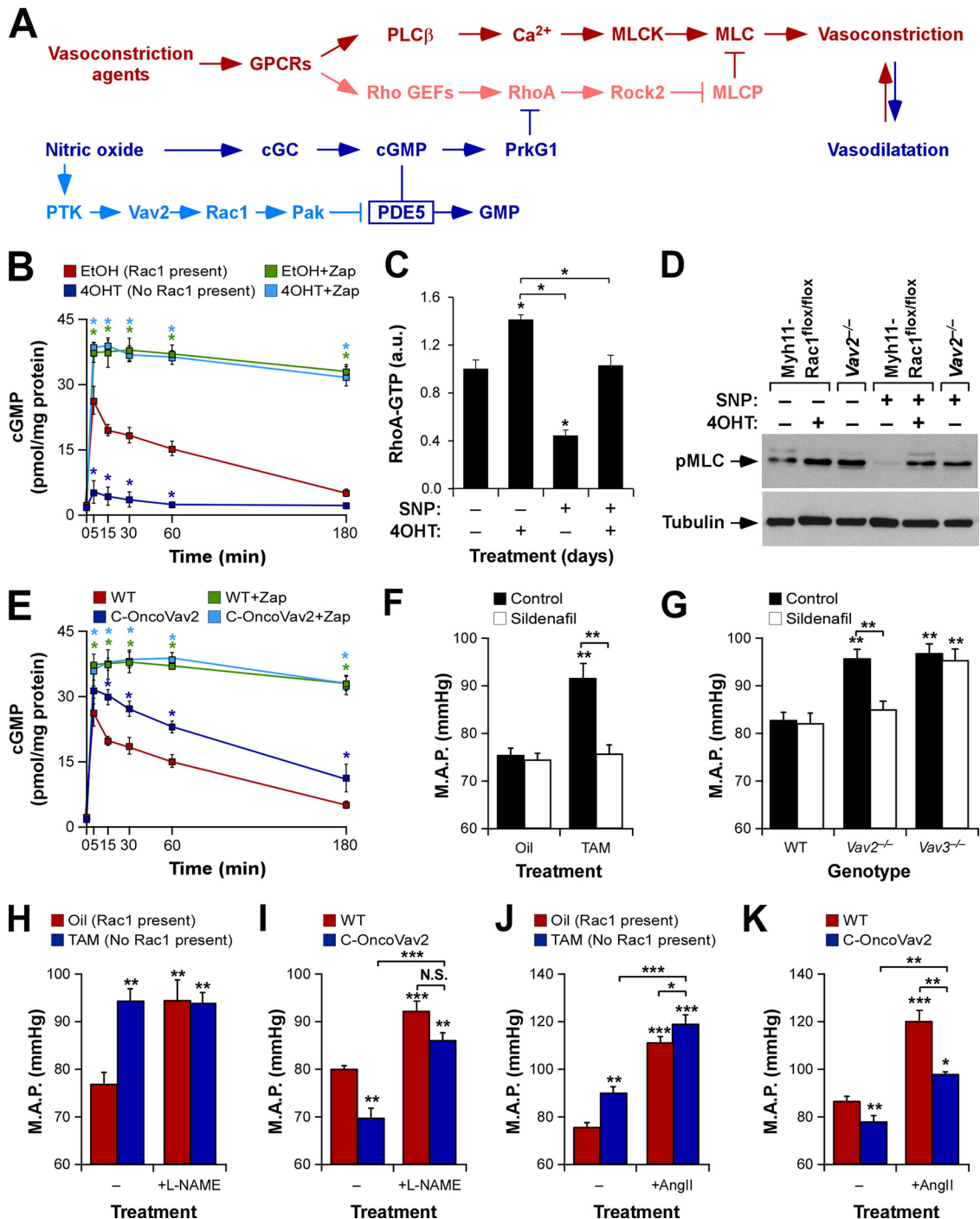
FIG 4 Vav2-Rac1 route is critical for the NO-mediated inhibition of RhoA-dependent contractile routes in vSMCs. (A) Scheme of signaling routes of vSMCs involved in vasoconstriction (red colors) and vasodilatation (blue colors) responses. GPCR, G protein-coupled receptor; PLCβ, phospholipase β; MLCK, MLC kinase; GEF, GDP/GTP exchange factor; MLCP, MLC phosphatase; sGC, soluble guanylate cyclase; PrkG1, protein kinase G1; PTK, protein tyrosine kinase; Pak, p21-associated kinase; PDE5, phosphodiesterase type 5. Further details are found in the text. (B) cGMP production by Myh11-Rac1$^{flox/flox}$ vSMC cells pretreated with the indicated chemicals and subsequently stimulated with SNP. EtOH, ethanol; Zap, Zaprinast. *, $P \leq 0.05$ relative to EtOH-treated cells (which express endogenous Rac1) ($n = 3$). (C) Amount of GTP-RhoA present in Myh11-Rac1$^{flox/flox}$ vSMC cells that were pretreated with 4OHT and stimulated with SNP as indicated. When 4OHT was not added, cells were pretreated with ethanol as described above. *, $P \leq 0.05$ relative to nonstimulated, EtOH-treated cells or the indicated experimental pair (in brackets) ($n = 4$). (D, upper) Representative immunoblot showing the amount of MLC phosphorylation in primary vSMCs from the indicated mice and culture conditions. (Lower) The amount of tubulin α was used as a loading control. Similar results were obtained in two additional independent experiments. (E) cGMP production by SNP-stimulated vSMC cells obtained from WT and C-OncoVav2 mice. When indicated, cells were pretreated with Zaprinast. *, $P \leq 0.05$ relative to SNP-stimulated WT cells ($n = 3$). (F and G) Mean arterial pressure present in Myh11-Rac1$^{flox/flox}$ (F) and *Vav* family knockout (G) mice subjected to the indicated treatments. Sildenafil was added in the drinking water for 1 week in each case before blood pressure evaluation. **, $P \leq 0.01$ compared to control mice or the indicated experimental pairs (in brackets) ($n = 4$ to 6). (H and I) Mean arterial pressure present in control (H and I), tamoxifen-treated Myh11-Rac1$^{flox/flox}$ (H), and C-OncoVav2 (I)

tent with the implication of this route in NO signaling, we observed that the *in vivo* administration of L-NAME, a NO synthase catalytic inhibitor that promotes hypertension through the inhibition of vSMC-dependent vasodilatation, promotes the elevation of the basal blood pressure of control mice, whereas it does not have any significant effect on the already hypertense tamoxifen-treated Myh11-Rac1$^{flox/flox}$ mice (Fig. 4H). In contrast, L-NAME-treated C-OncoVav2 mice do show a hypertensive response (Fig. 4I), indicating that the hyperactivation of the Vav2-Rac1 pathway does not confer any benefit under conditions of optimal ablation of nitric oxide signaling. These responses are L-NAME specific, because tamoxifen-treated Myh11-Rac1$^{flox/flox}$ mice do show enhanced pressor responses when systemically infused with AngII compared to controls (Fig. 4J). Conversely, C-OncoVav2 animals undergo milder pressor responses than control mice under these experimental conditions (Fig. 4K). Taken collectively, these findings confirm that the Vav2-Rac1 route is fully signaling autonomous to promote the inactivation of phosphodiesterase type 5 and effective nitric oxide vasodilation responses in vSMCs.

Rac1, but not Vav2, contributes to specific vascular remodeling events. We next investigated whether the Vav2-Rac1 signaling pathway present in vSMCs could be implicated in specific vascular-related pathologies. In contrast to previous inferences (1), we excluded the implication of Rac1 in hypertension-driven vascular remodeling, because the tamoxifen-treated Myh11-Rac1$^{flox/flox}$ mice showed no marked alterations in the thickening of arterial media walls typically seen under most systemic hypertension conditions (Fig. 2H) (1, 35). Vav2 is not involved either, because *Vav2*$^{-/-}$ (11, 17) and noninduced Myh11-OncoVav2 (Fabiano and Bustelo, unpublished) mice also show normal vascular remodeling upon developing hypertension. Similar results were found in *Vav3*$^{-/-}$ and *Vav2*$^{-/-}$; *Vav3*$^{-/-}$ mice (17, 18), ruling out that members of this family are in charge of this pathological process. To investigate the implications of these proteins in other vascular remodeling processes, we next performed neointima formation assays in both Myh11-Rac1$^{flox/flox}$ and standard *Vav2*$^{-/-}$ mice. To this end, we ligated one of the carotid arteries of these mice and, subsequently, measured the neointima formed in both proximal and distal histological cross sections of the ligated carotids. As a control, we analyzed similar sections from nonligated carotids. We found defective neointima formation in tamoxifen-treated Myh11-Rac1$^{flox/flox}$ (Fig. 5A and B) but not in *Vav2*$^{-/-}$ animals (Fig. 5C and D). Consistent with this, we observed, using both wound-healing and 3-(4,5-dimethylthiazol-2-yl)-2,5-diphenyltetrazolium bromide incorporation assays, that the 4OHT-induced depletion of Rac1 significantly reduced both the migration (Fig. 5E and F) and platelet-derived growth factor-induced proliferation (Fig. 5G) of primary vSMCs. *Vav2*$^{-/-}$ vSMCs behave exactly as their control counterparts in these two assays (Fig. 5E to G). However, the migration of vSMCs is Vav family dependent, because single *Vav3*$^{-/-}$ and compound *Vav2*$^{-/-}$; *Vav3*$^{-/-}$ vSMCs show ineffective wound-healing activity compared to controls (Fig. 5F). In contrast, the proliferation of vSMCs seems to be fully Vav independent (Fig. 5G). Taken to-

gether, these results indicate that the Rac1 route in vSMCs is important for both vascular tone regulation and neointima formation (Fig. 5H). In addition, they show that the activation of this GTPase in vSMCs requires the participation of different subsets of upstream exchange factors depending on the signaling route and biological process involved (Fig. 5H).

Rac1 signaling dysfunctions in vSMCs promote activation of systemic, prohypertensive pathophysiological programs in mice. In addition to the regulation of vascular tone, the development of a hypertensive state requires changes in renal and heart activities (1). Until now, however, it was rather difficult to establish the evolution in time of these physiological circuits upon a local dysfunction in vascular tone and to figure out how they are hierarchically organized during such a process. The availability of the tamoxifen-inducible Myh11-Rac1$^{flox/flox}$ mice offered us the opportunity to address this issue in a rather genetically and physiologically clean manner because, in this case, the depletion of this protein is circumscribed exclusively to SMCs. Perhaps more importantly, we believed that the use of this experimental model also could contribute to unveil potential synergisms between these vSMC extrinsic and intrinsic prohypertensive mechanisms that could favor the development and/or maintenance of the hypertensive state. To address those issues, we decided to monitor the evolution of blood pressure, heart activity, AngII, serotonin, catecholamines, and choline (an indirect readout for parasympathetic activity) upon vSMC-specific Rac1 depletion in Myh11-Rac1$^{flox/flox}$ mice. Given that some clinical data have linked peripheral vasoconstriction with the development of type 2 diabetes (36, 37), we included the evaluation of this parameter in our study. We found using that strategy that the first alteration observed in these mice is the elevation of blood pressure, since it is detected and reaches a plateau after just 1 week upon the termination of the tamoxifen treatments (Fig. 2E). Other alterations that take place rapidly upon tamoxifen treatment include the reduction in plasma levels of both choline (Fig. 6A) and serotonin (Fig. 6B). These changes are transient only in the case of serotonin (Fig. 6A and B). Although a known vasoconstrictor, plasma serotonin levels usually are downregulated in hypertensive conditions due to functional changes in platelets, the main reservoir of this substance in the blood (38). The elevation of AngII in plasma becomes statistically significant 2 weeks after the Rac1 depletion, reaching maximal amounts at the fourth posttreatment week (Fig. 6C). In contrast, the plasma concentrations of both noradrenaline (Fig. 6D) and adrenaline (Fig. 6E) become statistically significant only 4 weeks after the tamoxifen injections. The tachycardia found in these animals (Fig. 2G) develops and reaches maximal levels a week later than the hypertensive response (Fig. 6F). The increase in heart rate activity probably is initiated by the drop in parasympathetic activity, since it coincides with the time of reduction in the amount of choline in the plasma of these animals (Fig. 6A). Furthermore, it takes place several weeks before the upregulation of catecholamines in the system (Fig. 6D and E). In contrast, we could not detect any abnormal insulin-dependent response (Fig. 6G) or signs of metabolic syndrome in the liver (Fig. 6H and I),

---

mice that were either untreated (−) or treated (+L-NAME) with L-NAME for 1 week. $P \leq 0.01$ (**) and $P \leq 0.001$ (***) compared to either the appropriate control mice or the indicated experimental pairs (in brackets) ($n = 4$). N.S., not statistically significant. (J and K) Mean arterial pressure present in control (J and K), tamoxifen-treated Myh11-Rac1$^{flox/flox}$ (J), and C-OncoVav2 (K) mice upon the systemic infusion of AngII for 2 weeks. $P \leq 0.05$ (*), $P \leq 0.01$ (**), and $P \leq 0.001$ (***) compared to either the appropriate control mice or the indicated experimental pairs (in brackets) ($n = 4$). Error bars represent the SEM.
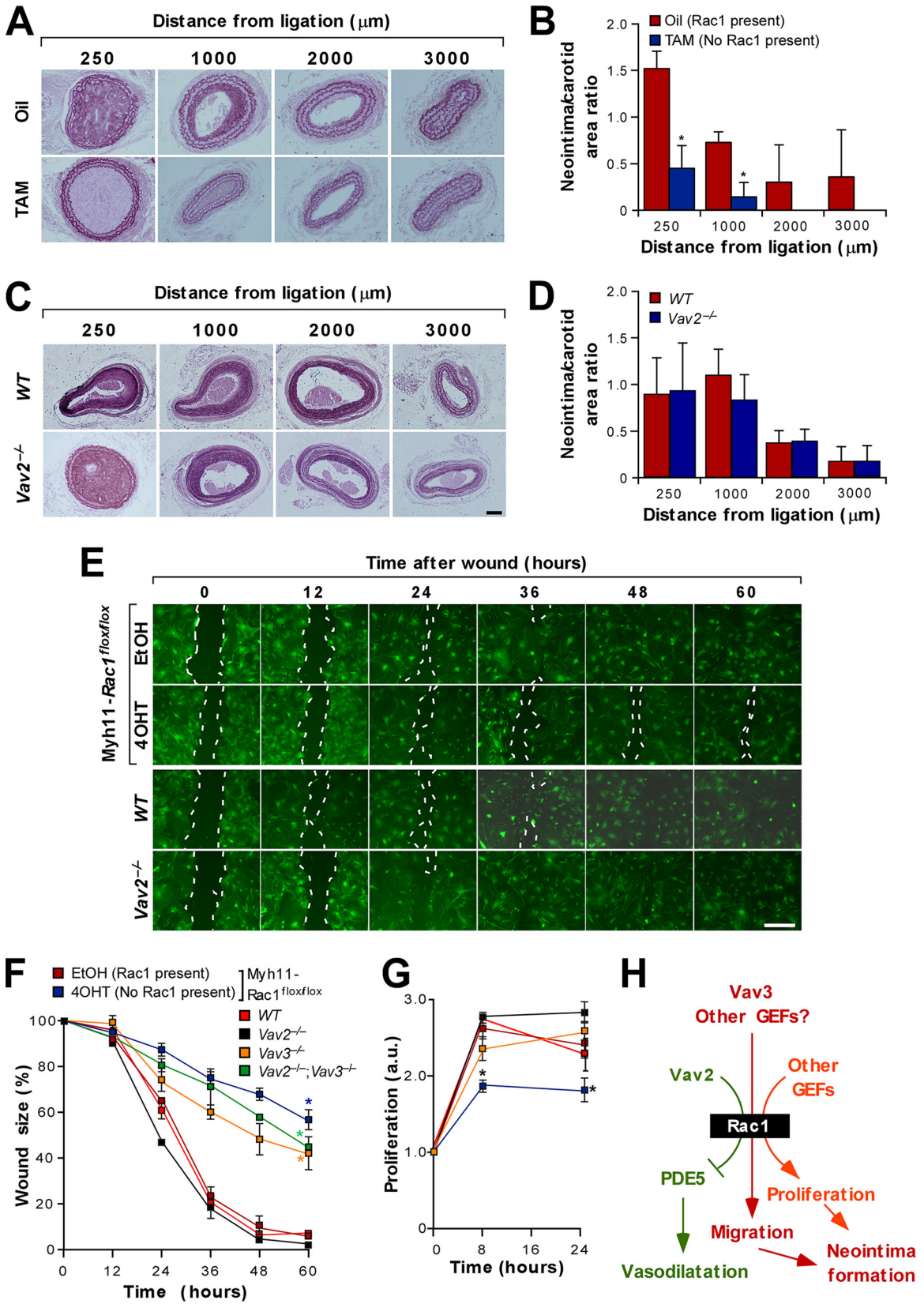
FIG 5 Rac1, but not Vav2, is important for vSMC-mediated neointima formation. (A and B) Representative images (A) (scale bar, 100 μm) and quantification (B) of neointima formation in Myh11-Rac1$^{flox/flox}$ mice 3 weeks after performing the tamoxifen-dependent recombination step. *, $P \leq 0.001$ relative to oil-injected mice in the same distance interval ($n = 4$). (C and D) Representative images (C) (scale bar, 100 μm) and quantification (D) of neointima formation in mice of the indicated genotypes ($n = 4$). Error bars represent the SEM. (E and F) Representative images (E) (scale bar, 10 μm)

white adipose tissue (Fig. 6H), and brown adipose tissue (Fig. 6H) in these animals. A summary of all of these pathophysiological changes is included in Fig. 7A.

vSMC signaling dysfunctions require cross talk with systemic vasopressor mechanisms to both induce and maintain hypertensive states. To investigate whether the pathophysiological changes observed in these mice were required to sustain the hypertensive phenotype of tamoxifen-treated Myh11-Rac1$^{flox/flox}$ mice, we next evaluated the effect that the serial administration of AngII biosynthesis (captopril) and nonselective β-adrenergic receptor (propranolol) inhibitors induced in the hypertension of these mice. Similar to the administration of sildenafil (Fig. 4F and 7B), we found that the transient treatment of these animals with captopril and propranolol results in the rapid elimination of the hypertensive state (Fig. 7A and B). This effect is abrogated when each of these drugs is removed (Fig. 7B). These three inhibitors exert the same antihypertensive effect when independently administered to tamoxifen-treated Myh11-Rac1$^{flox/flox}$ mice (Fig. 7C, left). Interestingly, we found that they also block the initial surge in blood pressure when administered both prior to and shortly after the gene recombination event (Fig. 7C, right). This suggests that the activation of the renin-AngII and sympathetic systems starts well before their systemic elevation in plasma. Local effects of the renin-AngII system in kidneys without concomitant elevations in plasma AngII levels have been found previously in L-NAME-triggered hypertension (39, 40). Importantly, this pathophysiological cadre seems to be fully dependent on the primary signaling dysfunction in vSMCs, as assessed by the rapid elimination of both the hypertension and tachycardia of Myh11-OncoVav2 mice upon the specific expression of OncoVav2 in vSMCs (Fig. 1D to F). Taken together, these findings indicate that the development and maintenance of the hypertension of Rac1-depleted mice requires the reciprocal cooperation of the intrinsic vSMC signaling defects and the extrinsic pathophysiological programs activated by them.

The renin-AngII system is key in the consolidation of the hypertensive phenotype induced by Rac1 depletion in vSMCs. The data described above indicated that the initial change in vascular tone derived from defective Rac1 signaling in vSMC requires the engagement of additional downstream physiological responses to generate a full-blown and stable hypertensive condition. Moreover, they suggested that this pathophysiological cadre evolves in a hierarchical manner, since the changes in the renin-AngII and parasympathetic systems are detected much earlier than those linked to the sympathetic nervous system. The stimulation of the renin-AngII system probably is one of the most important changes for the development of the hypertensive state of Myh11-Rac1$^{flox/flox}$ mice, because, in addition to the elimination of the hypertensive state (Fig. 7A to C), the *in vivo* administration of captopril eliminates the deregulated levels of heart activity, plasma choline, and plasma catecholamines present in tamoxifen-treated Myh11-Rac1$^{flox/flox}$ mice (Table 1 and Fig. 7A, Capt col-

umn). Consistent with this, we observed that the systemic administration of AngII to wild-type mice phenocopies the cardiovascular system-related pathophysiological dysfunctions seen in tamoxifen-treated Myh11-Rac1$^{flox/flox}$ mice (Table 1 and Fig. 7A, AngII column). The cardiovascular system-related effects elicited by AngII are seen even when coadministered with both α- and β-adrenergic receptor inhibitors (doxazosin and propranolol, respectively) (Table 1 and Fig. 7A, AngII+ARI column), indicating that they are caused by direct vasopressor effects of AngII rather than by indirect effects on the sympathoregulatory brain center. Unlike the case of AngII, we found that the systemic administration of the competitive inhibitor of parasympathetic-stimulated muscarinic acetylcholine receptors (atropine) recapitulates some (hypertension and tachycardia) but not all (increases in both AngII and noradrenaline) of the alterations previously seen in both tamoxifen-treated Myh11-Rac1$^{flox/flox}$ and AngII-treated C57BL/10 mice (Table 1 and Fig. 7A, Atr column).

DISCUSSION

Here, we have used a number of inducible and constitutive loss- and gain-of-function mouse models to address the intrinsic signaling roles of Vav family members and Rac1 in vSMCs. Our results indicate that Vav2 and Rac1, but not Cdc42 or RhoG (11), are involved in a linear pathway that controls, in a fully cell- and signaling-autonomous manner, NO- and phosphodiesterase type 5-dependent vasodilation responses in these cells. Unlike previous results (8–10), we have observed no vessel contractility defects in a large number of vasopressor substances in Rac1-depleted mesenteric arteries, indicating that this GTPase is not highly relevant for either the engagement or facilitation of vSMC contractility. It is possible that the discrepancy with some previous results reflects nonphysiological effects of Rac1 inhibitors and ectopically expressed Rac1 mutants used in those studies, or that such vasoconstriction roles could be circumscribed to pathological settings unrelated to normal arterial blood pressure control. The implication of the Vav2-Rac1 pathway in NO-dependent vSMC responses is quite interesting from a physiological point of view, because Rac1 is known to promote NO biosynthesis in endothelial cells (41–43). This suggests that Rac1 probably has been chosen during evolution as a common signaling hub to ensure the orchestration of fully coherent and optimal relaxation responses along the entire NO stimulation cycle of blood vessels. Whether Vav2 also plays roles in the regulation of NO production in endothelial cells remains to be determined. Our studies also have revealed that the Rac1 pathway is important for some but not all of the functions of vSMCs in vascular remodeling events. Consistent with this, we have seen that the thickening of the arterial media walls typically observed during hypertensive states develops normally in both Vav2- and Rac1-deficient mice. In contrast, we have found that Rac1 does play critical roles in neointima formation (Fig. 5H). This response is Vav2 independent, suggesting the presence of other exchange factors in this Rac1-dependent route (Fig. 5H).

and quantification (F) of the migration of primary Myh11-Rac1$^{flox/flox}$ (treated as indicated on the left, top two rows), Vav2$^{+/+}$ (WT; third row), and Vav2$^{-/-}$ (bottom row) vSMCs. In panel E, the experimental time points upon performing the wound are indicated at the top. The green fluorescence is from a fluorochrome incorporated into cells prior to the wound-healing experiment (see Materials and Methods). *, $P \leq 0.001$ relative to the appropriate control cell culture ($n = 3$). (G) Platelet-derived growth factor-induced proliferation of serum-starved vSMCs of the indicated genotypes. For color codes, see the inset in panel F. *, $P \leq 0.001$ relative to the appropriate control cell culture ($n = 3$). (H) Schematic representation of Rac1-dependent physiological (green color) and pathological (red colors) responses triggered by vSMCs. Upstream exchange factors (GEF) are indicated at the top.
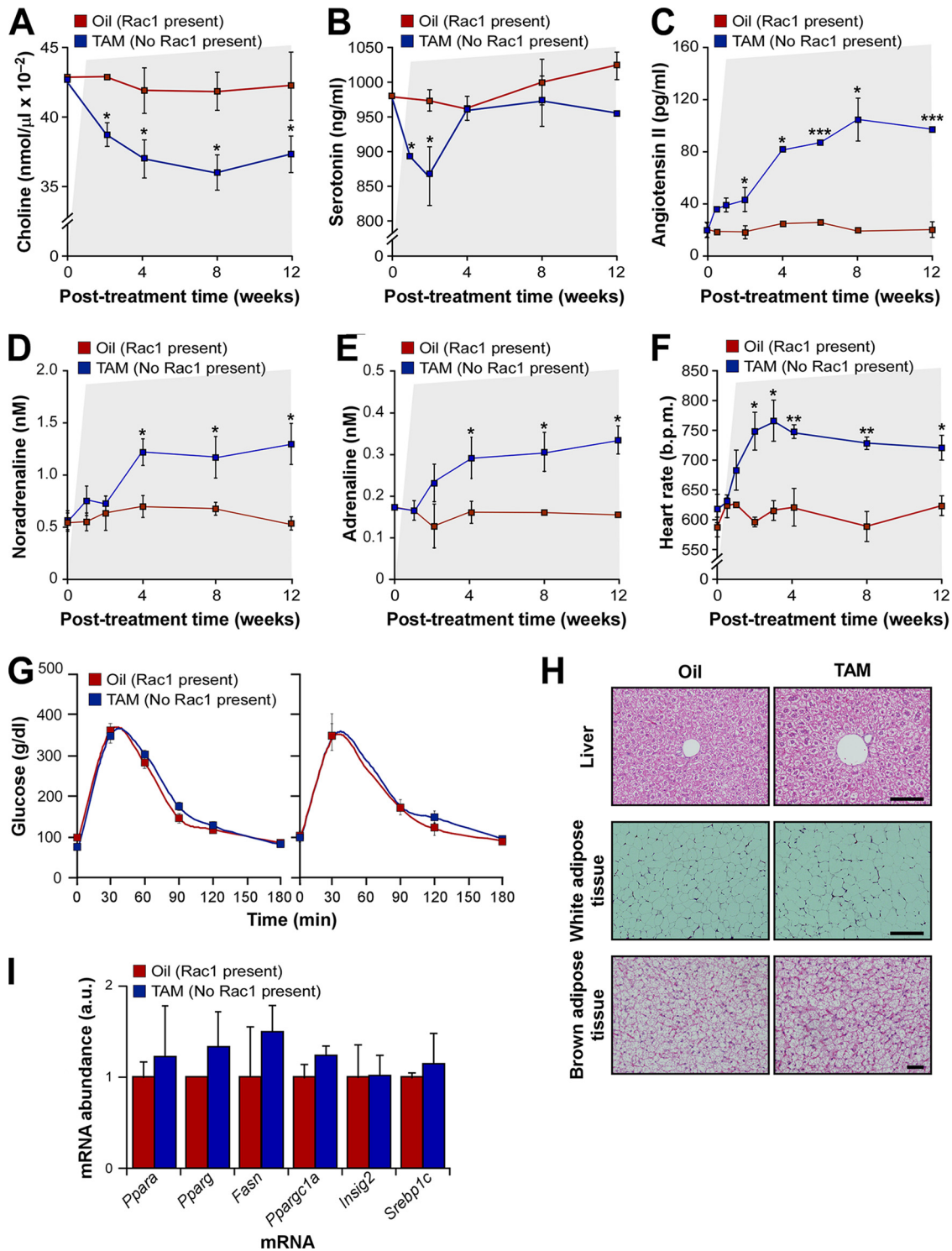
FIG 6 vSMC signaling dysfunctions require cross talk with downstream vasopressor mechanisms for hypertension development. (A to E) Evolution of the amount of plasma choline (A), serotonin (B), AngII (C), noradrenaline (D), and adrenaline (E) in Myh11-Rac1$^{flox/flox}$ mice upon the final injections with either oil or tamoxifen. This time point was considered 0. The periods associated with hypertension conditions (see the legend to Fig. 2D) are indicated as shaded areas in all panels. $P \leq 0.05$ (*) and $P \leq 0.001$ (***) compared to oil-injected mice ($n = 4$). (F) Evolution of the heart rates in the same animals and experimental conditions. Periods of hypertension are indicated. $P \leq 0.05$ (*) and $P \leq 0.01$ (**) compared to oil-injected mice ($n = 4$). (G) Plasma glucose concentration upon glucose injection in mice 2 (left) and 3 (right) months after final injections with either oil or tamoxifen ($n = 4$ and 5 for oil- and tamoxifen-treated mice, respectively). (H) Representative images of hematoxylin-eosin-stained sections from the indicated tissues (left) derived from 4-month-old Myh11-Rac1$^{flox/flox}$ mice 3 months after either the oil or tamoxifen injections (top). Scale bars, 100 μm. No signs of steatosis (top) or hypertrophy of white (middle) or brown (bottom) adipocytes are seen ($n = 4$ and 5 for oil- and tamoxifen-treated mice, respectively). (I) Abundance of the indicated mRNAs typically associated with hepatic steatosis in livers obtained from 4-month-old mice treated as described for panel G ($n = 4$ and 5 for oil- and tamoxifen-treated mice, respectively). Error bars represent the SEM.
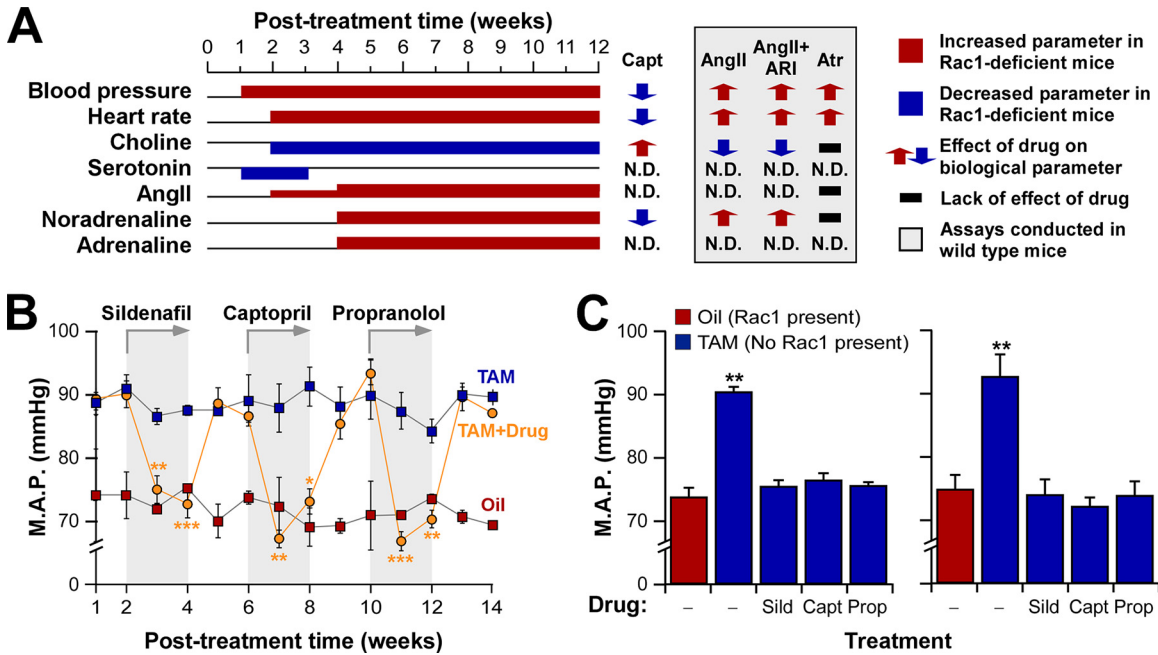
FIG 7 Renin-angiotensin II and sympathetic systems are required to maintain the hypertension of Myh11-Rac1[flox/flox] mice. (A) Summary of the evolution of indicated physiological parameters and regulatory molecules (left) in Myh11-Rac1[flox/flox] mice upon the tamoxifen-induced recombination step in the *Rac1* locus (data are derived from those shown in Fig. 6). Upregulated (red boxes on basal lane) and downregulated (blue boxes underneath basal lane) responses are indicated. The time after the recombination step is indicated at the top. Effects induced by the indicated drug treatments on either tamoxifen-treated Myh11-Rac1[flox/flox] (Capt column) or wild-type (AngII, AngII+ARI, and Atr columns) mice are also shown (see the box on the right for other symbols used in this panel). Capt, captopril; ARI, adrenergic receptor inhibitors; Atr, atropine; N.D., not determined. (B) Evolution of mean arterial pressure of tamoxifen-treated Myh11-Rac1[flox/flox] mice upon the indicated drug treatments. A shaded area indicates the time of administration of each drug. As a control, we included the mean arterial pressure of control, oil-injected Myh11-Rac1[flox/flox] mice. $P \leq 0.05$ (*), $P \leq 0.01$ (**), and $P \leq 0.001$ (***) relative to oil-injected mice at the indicated experimental time points ($n = 4$). (C, left) Mean arterial pressure of Myh11-Rac1[flox/flox] mice that, 4 weeks after the injections with tamoxifen, were treated with the indicated drugs for 1 week. (Right) Mean arterial pressure of Myh11-Rac1[flox/flox] mice treated with the indicated treatments before and after being injected with either oil or tamoxifen. Recordings were done 1 week after the indicated injections. In both cases, we include for comparison the arterial pressure values of control mice simply injected with oil. Sild, sildenafil; Prop, propranolol. **, $P \leq 0.01$ relative to oil-injected mice ($n = 4$). Error bars represent the SEM.

Possible candidates include ArhGEF7 and Kalirin, since these exchange factors promote the proliferation and migration of vSMC *in vitro* and, in the case of Kalirin, neointima formation *in vivo* (44, 45). Our results suggest that Vav3 also can represent a good candidate for this regulatory step (Fig. 5H). Unfortunately, we could not verify this possibility, because all *Vav3*^{-/-} mice used in neointima experiments died shortly after the ligation step of the carotid (M. A. Sevilla, S. Fabbiano, M. J. Montero, and X. R. Bustelo, unpublished data). The cause for this mortality is unknown,

although it may be due to the chronic sympathoexcitation present in these mice (18, 34).

The inducible nature of some of the mouse models used in this study also has allowed us to recapitulate, in a genetically and physiological "clean" manner, the alterations that take place at the organism level upon a single vascular tone-related signaling defect in vSMCs. We have observed that such alterations include, among others, the progressive stimulation of both the renin-AngII and sympathetic nervous systems (Fig. 7A). The combined activation

TABLE 1 Effect of indicated treatments on Myh-Rac1[flox/flox] and wild-type C57BL/10 mice

Parameter	Value according to mouse strain and treatment[a]						
	Myh11-Rac1[flox/flox]			C57BL/10			
	Oil	Tamoxifen	Tamoxifen and captopril	Control	AngII	AngII, Prop, and Doxa[b]	Atropine
M.A.P. (mmHg)	74 ± 2	87 ± 3*	72 ± 2#	78 ± 4	112 ± 3*	116 ± 4*	97 ± 2*
Heart rate (bpm)	603 ± 12	709 ± 18*	570 ± 9#	594 ± 11	697 ± 38*	712 ± 24*	722 ± 15*
AngII (pg/ml)	30 ± 1	97 ± 5*	ND	32 ± 3	ND	ND	39 ± 5
Choline (nmol/μl)	0.032 ± 0.01	0.026 ± 0.00*	0.036 ± 0.00#	0.034 ± 0.00	0.024 ± 0.00*	0.023 ± 0.00*	0.028 ± 0.01
Noradrenaline (nM)	0.88 ± 0.12	1.48 ± 0.14*	0.66 ± 0.05#	0.62 ± 0.12	1.72 ± 0.22*	1.54 ± 0.3*	0.67 ± 0.12

[a] See Materials and Methods for details about treatments performed. *, $P \leq 0.05$ compared to the appropriate untreated control; #, $P \leq 0.05$ compared to tamoxifen-treated mice. ND, not determined.
[b] Prop, propranolol; Doxa, doxazosine.

of these two systems probably favors the evasion of the renal pressure-natriuresis mechanism that ensures the long-term arterial pressure homeostasis and, subsequently, the aggravation of the hypertensive state through the cardiac-, vasopressor-, and vascular remodeling-mediated increase in peripheral arterial resistance (46). These two systems become activated very early upon Rac1 deletion, because captopril and propranolol can halt the development of hypertension even when administered prior to the gene recombination event and during short postrecombination periods in which AngII and catecholamines have not yet reached systemic levels in plasma. We have also found a very early reduction of parasympathetic activity that contributes to the early tachycardic response seen right after the Rac1 depletion in vSMCs and, in addition, to the increased vasoconstriction present in these mice (Fig. 7A). The latter response is probably a physiological adaptation to elevated blood pressure conditions, since it also has been observed both in the neurogenic hypertension conditions exhibited by $Vav3^{-/-}$ mice (26) and during the systemic administration of AngII to wild-type mice (Table 1). Taken together, our results indicate that the local dysfunction of Vav2 and Rac1 signaling in vSMCs elicits a butterfly effect that eventually leads to the generation of a general prohypertensive pathophysiological status in animals. In contrast, we observed that mice depleted of Rac1 in vSMCs do not develop type 2 diabetes even after long periods of chronic hypertension and high AngII levels in plasma. This is intriguing, because multiple clinical studies have shown associations between the development of this disease and the presence of either chronic vasoconstriction or systemic AngII conditions (36, 37). It has been argued that such linkages are due to direct effects of the above-described cardiovascular parameters on insulin responses. Proposed models include negative effects induced by vasoconstriction itself in the availability of both glucose and insulin in peripheral tissues, intrinsic signaling effects of AngII in pancreatic cells, and negative influences of AngII-stimulated pathways on insulin receptor downstream signaling elements in a number of cell types (36, 37). However, other studies favor the concept that such association reflects an ancillary function of those cardiovascular parameters in individuals that are already predisposed to develop type 2 diabetes (37). Answering this issue has been difficult so far in humans given the multiple gender, ethnic, metabolic, and lifestyle variables involved in the development of all of these diseases. Our results tilt the balance in favor of the latter model, since they suggest that chronic hypertension and high AngII conditions are not sufficient *per se* to trigger glucose tolerance or type 2 diabetes in the absence of such a genetic predisposition, at least in the case of mice.

The present results also suggest that the pharmacological inhibition of Rac1 will lead to the inexorable development of hypertension and its typical comorbidities. This observation is particularly important given the intensive efforts that currently are being made to isolate specific inhibitors for exchange factors, exchange factor-Rac1 interactions, and the catalytic activity of p21-activated kinase family members to treat cancer patients (47, 48). However, our results also indicate that these side effects will be readily eliminated upon the removal of those therapies or, perhaps more importantly, fully prevented when using them in combination with standard antihypertension treatments already utilized in clinical practice.

REFERENCES

1. **Loirand G, Sauzeau V, Pacaud P.** 2013. Small G proteins in the cardiovascular system: physiological and pathological aspects. Physiol. Rev. **93:** 1659–1720. http://dx.doi.org/10.1152/physrev.00021.2012.

2. **Gong L, Pitari GM, Schulz S, Waldman SA.** 2004. Nitric oxide signaling: systems integration of oxygen balance in defense of cell integrity. Curr. Opin. Hematol. **11:**7–14. http://dx.doi.org/10.1097/00062752-200401000-00003.

3. **Hofmann F, Feil R, Kleppisch T, Schlossmann J.** 2006. Function of cGMP-dependent protein kinases as revealed by gene deletion. Physiol. Rev. **86:**1–23. http://dx.doi.org/10.1152/physrev.00015.2005.

4. **Sauzeau V, Le Jeune H, Cario-Toumaniantz C, Smolenski A, Lohmann SM, Bertoglio J, Chardin P, Pacaud P, Loirand G.** 2000. Cyclic GMP-dependent protein kinase signaling pathway inhibits RhoA-induced Ca2+ sensitization of contraction in vascular smooth muscle. J. Biol. Chem. **275:**21722–21729. http://dx.doi.org/10.1074/jbc.M000753200.

5. **Omori K, Kotera J.** 2007. Overview of PDEs and their regulation. Circ. Res. **100:**309–327. http://dx.doi.org/10.1161/01.RES.0000256354.95791.f1.

6. **Bustelo XR, Sauzeau V, Berenjeno IM.** 2007. GTP-binding proteins of the Rho/Rac family: regulation, effectors and functions in vivo. Bioessays **29:**356–370. http://dx.doi.org/10.1002/bies.20558.

7. **Jaffe AB, Hall A.** 2005. Rho GTPases: biochemistry and biology. Annu. Rev. Cell Dev. Biol. **21:**247–269. http://dx.doi.org/10.1146/annurev.cellbio.21.020604.150721.

8. **Foster DB, Shen LH, Kelly J, Thibault P, Van Eyk JE, Mak AS.** 2000. Phosphorylation of caldesmon by p21-activated kinase. Implications for the Ca(2+) sensitivity of smooth muscle contraction. J. Biol. Chem. **275:** 1959–1965. http://dx.doi.org/10.1074/jbc.275.3.1959.

9. **Rahman A, Davis B, Lovdahl C, Hanumaiah VT, Feil R, Brakebusch C, Arner A.** 2014. The small GTPase Rac1 is required for smooth muscle contraction. J. Physiol. **592:**915–926. http://dx.doi.org/10.1113/jphysiol.2013.262998.

10. **Hassanain HH, Gregg D, Marcelo ML, Zweier JL, Souza HP, Selvakumar B, Ma Q, Moustafa-Bayoumi M, Binkley PF, Flavahan NA, Morris M, Dong C, Goldschmidt-Clermont PJ.** 2007. Hypertension caused by transgenic overexpression of Rac1. Antioxid. Redox Signal. **9:**91–100. http://dx.doi.org/10.1089/ars.2007.9.91.

11. **Sauzeau V, Sevilla MA, Montero MJ, Bustelo XR.** 2010. The Rho/Rac exchange factor Vav2 controls nitric oxide-dependent responses in mouse vascular smooth muscle cells. J. Clin. Investig. **120:**315–330. http://dx.doi.org/10.1172/JCI38356.

12. **Wirth A, Schroeter M, Kock-Hauser C, Manser E, Chalovich JM, De Lanerolle P, Pfitzer G.** 2003. Inhibition of contraction and myosin light chain phosphorylation in guinea-pig smooth muscle by p21-activated kinase 1. J. Physiol. **549:**489–500. http://dx.doi.org/10.1113/jphysiol.2002.033167.

13. **Bustelo XR.** 2000. Regulatory and signaling properties of the Vav family.

Mol. Cell. Biol. **20**:1461–1477. http://dx.doi.org/10.1128/MCB.20.5.1461 -1477.2000.

14. **Schuebel KE, Movilla N, Rosa JL, Bustelo XR.** 1998. Phosphorylation-dependent and constitutive activation of Rho proteins by wild-type and oncogenic Vav-2. EMBO J. **17**:6608–6621. http://dx.doi.org/10.1093 /emboj/17.22.6608.

15. **Turner M, Billadeau DD.** 2002. VAV proteins as signal integrators for multi-subunit immune-recognition receptors. Nat. Rev. Immunol. **2**:476–486. http://dx.doi.org/10.1038/nri840.

16. **Bond M, Wu YJ, Sala-Newby GB, Newby AC.** 2008. Rho GTPase, Rac1, regulates Skp2 levels, vascular smooth muscle cell proliferation, and intima formation in vitro and in vivo. Cardiovasc. Res. **80**:290–298. http: //dx.doi.org/10.1093/cvr/cvn188.

17. **Sauzeau V, Jerkic M, Lopez-Novoa JM, Bustelo XR.** 2007. Loss of Vav2 proto-oncogene causes tachycardia and cardiovascular disease in mice. Mol. Biol. Cell **18**:943–952. http://dx.doi.org/10.1091/mbc.E06-09-0877.

18. **Sauzeau V, Sevilla MA, Rivas-Elena JV, de Alava E, Montero MJ, Lopez-Novoa JM, Bustelo XR.** 2006. Vav3 proto-oncogene deficiency leads to sympathetic hyperactivity and cardiovascular dysfunction. Nat. Med. **12**:841–845. http://dx.doi.org/10.1038/nm1426.

19. **Doody GM, Bell SE, Vigorito E, Clayton E, McAdam S, Tooze R, Fernandez C, Lee IJ, Turner M.** 2001. Signal transduction through Vav-2 participates in humoral immune responses and B cell maturation. Nat. Immunol. **2**:542–547. http://dx.doi.org/10.1038/88748.

20. **Yang L, Wang L, Zheng Y.** 2006. Gene targeting of Cdc42 and Cdc42GAP affirms the critical involvement of Cdc42 in Filopodia induction, directed migration, and proliferation in primary mouse embryonic fibroblasts. Mol. Biol. Cell **17**:4675–4685. http://dx.doi.org/10.1091/mbc.E06-05-0466.

21. **Wirth A, Benyo Z, Lukasova M, Leutgeb B, Wettschureck N, Gorbey S, Orsy P, Horvath B, Maser-Gluth C, Greiner E, Lemmer B, Schutz G, Gutkind JS, Offermanns S.** 2008. G12-G13-LARG-mediated signaling in vascular smooth muscle is required for salt-induced hypertension. Nat. Med. **14**:64–68. http://dx.doi.org/10.1038/nm1666.

22. **Citterio C, Menacho-Marquez M, Garcia-Escudero R, Larive RM, Barreiro O, Sanchez-Madrid F, Paramio JM, Bustelo XR.** 2012. The Rho exchange factors Vav2 and Vav3 control a lung metastasis-specific transcriptional program in breast cancer cells. Sci. Signal. **5**:ra71. http://dx.doi .org/10.1126/scisignal.2002962.

23. **Castro-Castro A, Ojeda V, Barreira M, Sauzeau V, Navarro-Lerida I, Muriel O, Couceiro JR, Pimentel-Muinos FX, Del Pozo MA, Bustelo XR.** 2011. Coronin 1A promotes a cytoskeletal-based feedback loop that facilitates Rac1 translocation and activation. EMBO J. **30**:3913–3927. http: //dx.doi.org/10.1038/emboj.2011.310.

24. **Castro-Castro A, Ojeda V, Barreira M, Sauzeau V, Navarro-Lerida I, Muriel O, Couceiro JR, Pimentel-Muinos FX, Del Pozo MA, Bustelo XR.** 2011. Coronin 1A promotes a cytoskeletal-based feedback loop that facilitates Rac1 translocation and activation. EMBO J. **30**:3913–3927. http: //dx.doi.org/10.1038/emboj.2011.310.

25. **Althoff TF, Albarran Juarez J, Troidl K, Tang C, Wang S, Wirth A, Takefuji M, Wettschureck N, Offermanns S.** 2012. Procontractile G protein-mediated signaling pathways antagonistically regulate smooth muscle differentiation in vascular remodeling. J. Exp. Med. **209**:2277–2290. http://dx.doi.org/10.1084/jem.20120350.

26. **Menacho-Marquez M, Nogueiras R, Fabbiano S, Sauzeau V, Al-Massadi O, Dieguez C, Bustelo XR.** 2013. Chronic sympathoexcitation through loss of Vav3, a Rac1 activator, results in divergent effects on metabolic syndrome and obesity depending on diet. Cell Metab. **18**:199–211. http://dx.doi.org/10.1016/j.cmet.2013.07.001.

27. **Movilla N, Bustelo XR.** 1999. Biological and regulatory properties of Vav-3, a new member of the Vav family of oncoproteins. Mol. Cell. Biol. **19**:7870–7885.

28. **Zugaza JL, Lopez-Lago MA, Caloca MJ, Dosil M, Movilla N, Bustelo XR.** 2002. Structural determinants for the biological activity of Vav proteins. J. Biol. Chem. **277**:45377–45392. http://dx.doi.org/10.1074 /jbc.M208039200.

29. **Barreira M, Fabbiano S, Couceiro JR, Torreira E, Martinez-Torrecuadrada JL, Montoya G, Llorca O, Bustelo XR.** 2014. The C-terminal SH3 domain contributes to the intramolecular inhibition of Vav family proteins. Sci. Signal. **7**:ra35. http://dx.doi.org/10.1126/scisignal.2004993.

30. **Gu Y, Filippi MD, Cancelas JA, Siefring JE, Williams EP, Jasti AC, Harris CE, Lee AW, Prabhakar R, Atkinson SJ, Kwiatkowski DJ, Williams DA.** 2003. Hematopoietic cell regulation by Rac1 and Rac2 guanosine triphosphatases. Science **302**:445–449. http://dx.doi.org/10 .1126/science.1088485.

31. **Furchgott RF, Zawadzki JV.** 1980. The obligatory role of endothelial cells in the relaxation of arterial smooth muscle by acetylcholine. Nature **288**: 373–376. http://dx.doi.org/10.1038/288373a0.

32. **Napoli C, Ignarro LJ.** 2003. Nitric oxide-releasing drugs. Annu. Rev. Pharmacol. Toxicol. **43**:97–123. http://dx.doi.org/10.1146/annurev.pharmtox.43 .100901.140226.

33. **Corbin JD, Francis SH.** 1999. Cyclic GMP phosphodiesterase-5: target of sildenafil. J. Biol. Chem. **274**:13729–13732. http://dx.doi.org/10.1074/jbc .274.20.13729.

34. **Sauzeau V, Horta-Junior JAC, Riolobos AS, Fernandez G, Sevilla MA, Lopez DE, Montero MJ, Rico B, Bustelo XR.** 2010. Vav3 is involved in GABAergic axon guidance events important for the proper function of brainstem neurons controlling cardiovascular, respiratory, and renal parameters. Mol. Biol. Cell **21**:4251–4263. http://dx.doi.org/10.1091/mbc .E10-07-0639.

35. **Staessen JA, Wang J, Bianchi G, Birkenhager WH.** 2003. Essential hypertension. Lancet **361**:1629–1641. http://dx.doi.org/10.1016/S0140-6736(03)13302-8.

36. **Mancia G, Bousquet P, Elghozi JL, Esler M, Grassi G, Julius S, Reid J, Van Zwieten PA.** 2007. The sympathetic nervous system and the metabolic syndrome. J. Hypertens. **25**:909–920. http://dx.doi.org/10 .1097/HJH.0b013e328048d004.

37. **Ando K, Fujita T.** 2006. Anti-diabetic effect of blockade of the renin-angiotensin system. Diabetes Obes. Metab. **8**:396–403. http://dx.doi.org /10.1111/j.1463-1326.2005.00526.x.

38. **Watts SW, Morrison SF, Davis RP, Barman SM.** 2012. Serotonin and blood pressure regulation. Pharmacol. Rev. **64**:359–388. http://dx.doi.org /10.1124/pr.111.004697.

39. **Pollock DM, Polakowski JS, Divish BJ, Opgenorth TJ.** 1993. Angiotensin blockade reverses hypertension during long-term nitric oxide synthase inhibition. Hypertension **21**:660–666. http://dx.doi.org/10.1161/01.HYP .21.5.660.

40. **Rees DD, Palmer RM, Moncada S.** 1989. Role of endothelium-derived nitric oxide in the regulation of blood pressure. Proc. Natl. Acad. Sci. U. S. A. **86**:3375–3378. http://dx.doi.org/10.1073/pnas.86.9.3375.

41. **Gonzalez E, Kou R, Michel T.** 2006. Rac1 modulates sphingosine 1-phosphate-mediated activation of phosphoinositide 3-kinase/Akt signaling pathways in vascular endothelial cells. J. Biol. Chem. **281**:3210–3216. http: //dx.doi.org/10.1074/jbc.M510434200.

42. **Sawada N, Salomone S, Kim HH, Kwiatkowski DJ, Liao JK.** 2008. Regulation of endothelial nitric oxide synthase and postnatal angiogenesis by Rac1. Circ. Res. **103**:360–368. http://dx.doi.org/10.1161/CIRCRESAHA.108 .178897.

43. **Levine YC, Li GK, Michel T.** 2007. Agonist-modulated regulation of AMP-activated protein kinase (AMPK) in endothelial cells. Evidence for an AMPK→Rac1→Akt→ endothelial nitric-oxide synthase pathway. J. Biol. Chem. **282**:20351–20364. http://dx.doi.org/10.1074/jbc .M702182200.

44. **Shin EY, Lee CS, Park MH, Kim DJ, Kwak SJ, Kim EG.** 2009. Involvement of betaPIX in angiotensin II-induced migration of vascular smooth muscle cells. Exp. Mol. Med. **41**:387–396. http://dx.doi.org/10.3858/emm .2009.41.6.044.

45. **Wu JH, Fanaroff AC, Sharma KC, Smith LS, Brian L, Eipper BA, Mains RE, Freedman NJ, Zhang L.** 2013. Kalirin promotes neointimal hyperplasia by activating Rac in smooth muscle cells. Arterioscler. Thromb. Vasc. Biol. **33**:702–708. http://dx.doi.org/10.1161/ATVBAHA.112.300234.

46. **Cowley AW, Jr.** 1992. Long-term control of arterial blood pressure. Physiol. Rev. **72**:231–300.

47. **Vigil D, Cherfils J, Rossman KL, Der CJ.** 2010. Ras superfamily GEFs and GAPs: validated and tractable targets for cancer therapy? Nat. Rev. Cancer **10**:842–857. http://dx.doi.org/10.1038/nrc2960.

48. **Radu M, Semenova G, Kosoff R, Chernoff J.** 2014. PAK signalling during the development and progression of cancer. Nat. Rev. Cancer **14**:13–25. http://dx.doi.org/10.1038/nrc3645.